NASA Contractor Report 3602

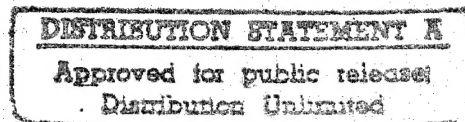DTIC
SELECTED
JAN 0 5 1996
F

Test and Analysis of Celion 3000/PMR-15, Graphite/Polyimide Bonded Composite Joints

Summary

19960103 181

J. B. Cushman, S. F. McCleskey,
and S. H. Ward

NASA

DTIC DOES NOT HAVE THIS ITEM

--- 1 --- AD NUMBER: D436360
--- 5 --- CORPORATE AUTHOR: BOEING AEROSPACE CO SEATTLE WA
--- 6 --- UNCLASSIFIED TITLE: TEST AND ANALYSIS OF CELION 3000/PMR-15,
---   GRAPHITE/POLYIMIDE BONDED COMPOSITE JOINTS—SUMMARY,
---10 --- PERSONAL AUTHORS: CUSHMAN,J. B. ;MCCLESKEY,S. F. ;WARD,S. H. ;
---11 --- REPORT DATE: JAN , 1983
---12 --- PAGINATION: 78P
---15 --- CONTRACT NUMBER: NAS1-15644
---18 --- MONITOR ACRONYM: NASA
---19 --- MONITOR SERIES: CR-3602
---20 --- REPORT CLASSIFICATION: UNCLASSIFIED
---22 --- LIMITATIONS (ALPHA):   APPROVED FOR PUBLIC RELEASE; DISTRIBUTION
---   UNLIMITED. AVAILABILITY: NATIONAL TECHNICAL INFORMATION SERVICE,
---   SPRINGFIELD, VA. 22161. NASA-CR-3602.
---33 --- LIMITATION CODES: 1 24

NASA Contractor Report 3602

Test and Analysis of Celion 3000/PMR-15, Graphite/Polyimide Bonded Composite Joints

Summary

J. B. Cushman, S. F. McCleskey,
and S. H. Ward
Boeing Aerospace Company
Seattle, Washington

NASA

National Aeronautics
and Space Administration

**Scientific and Technical
Information Branch**

1983

FOREWORD

This document was prepared by the Boeing Aerospace Company for the National Aeronautics and Space Administration, Langley Research Center in compliance with Contract NAS1-15644, "Design, Fabrication and Test of Graphite/Polyimide Composite Joints and Attachments for Advanced Aerospace Vehicles."

This report is one of five that fully document contract results. It is the Summary of the Task 2.0 "Bonded Joint Tests."

Dr. Paul A. Cooper was the contracting officer's technical representative for the full contract and Gregory Wichorek was the technical representative for design allowables testing of Celion 6000/PMR-15. Boeing performance was under the management of Mr. J. E. Harrison. Mr. D. E. Skoumal was the technical leader. Major participants in this program were Stephen H. Ward, Stephen F. McCleskey and James B. Cushman, Structural Development and Sylvester G. Hill, Materials and Processes.

Certain materials are identified in this publication in order to specify adequately which materials were investigated. In no case does such identification imply recommendation or endorsement of the material by NASA, nor does it imply that the materials are necessarily the only ones or the best ones available for the purpose.

ii

TABLE OF CONTENTS

THIS PAGE INTENTIONALLY LEFT BLANK

iv

LIST OF FIGURES

LIST OF FIGURES (Continued)

Number	TITLE	Page

LIST OF TABLES

THIS PAGE INTENTIONALLY LEFT BLANK

1.0 SUMMARY

This report summarizes a test/analysis program of bonded composite joints conducted for NASA under Contract NAS1-15644. The objective of the program was to establish a limited data base describing the influence of variations in basic design parameters on the static strength and failure modes of graphite/polyimide (Gr/PI) bonded joints for use at elevated temperatures.

An initial literature search was conducted to seek experimental data and analyses concerned with standard bonded joints. While various research programs have dealt with epoxy bonded metal and epoxy bonded composite joints, few programs featuring polyimide materials and specifically bonded graphite/polyimide composites were found in the open literature.

A test plan was developed to investigate the effect of geometric and material parameters and elevated temperature on the static strength of "standard" joints. Single-lap and double-lap composite joints, and single-, double- and step-lap composite to metal joints were characterized. Tests were also conducted to measure shear strength, shear modulus and flatwise tension strength of the chosen adhesive system.

Finite element analyses were conducted to evaluate modeling techniques and to assess effects of lamina stacking sequence and adhesive filleting on single- and double-lap bonded composite joints.

Test specimens were fabricated from a Gr/PI system: Celion 3000 graphite fiber and PMR-15 polyimide resin. Joint bonding utilized a LARC-13 modified adhesive designated A7F. A total of 653 tests were conducted to evaluate effects of lap length, adherend thickness, adherend axial stiffness, lamina stacking sequence and adherend tapering. All specimens were subjected to a conditioning of 125 hours at 589K (600°F) prior to testing at 116K (-250°F), 294K (70°F), and 561K (550°F).

An additional test matrix of "advanced" joints was established based on the results of the "standard" tests. The advanced joints, consisting of preformed adherends, adherends with scalloped edges and joints with hybrid interface plies, were tested and compared to baseline single- and double-lap designs.

Test results indicated that single-lap joints can be designed and fabricated that will carry 123 to 385 kN/m (700 to 2200 lb/in.) at 561K (550°F) and double-lap and symmetric step-lap attachments would be effective in the 438 to 875 kN/m (2500-5000 lb/in) range at 561K (550°F). The predominate failure mode was intralaminar shear and peel of the composite. The few adhesive failures that occurred were primarily on the high temperature tests of the composite-to-titanium joints.

The "advanced" joint tests indicated that a significant improvement in joint efficiency is available through geometric modifications and hybrid material additions at the adherend interfaces.

Correlation of test results for single lap composite-to-composite joints and to a limited degree for the titanium step-lap joints was achieved with closed form analytical models. Empirical correlations were developed for single-and double-lap joints.

2.0 INTRODUCTION

Advanced designs for high-speed aircraft and space transportation systems require more efficient structures for operation in the 116K (-250°F) to 589K (600°F) temperature range. Design data are needed for bonded and bolted composite joints to support advanced design concepts. An experimental program to evaluate several concepts of graphite/polymide (Gr/PI) bonded and bolted joints was funded under NASA contract NAS1-15644.

The program was designed to extend the current epoxy-matrix composite technology in joint and attachment design to include high-temperature polymide matrix composites. It provides an initial data base for designing and fabricating Gr/PI lightly loaded control surface structures for advanced space transportation systems and high-speed aircraft. The objectives of this program were two-fold: first, to identify and evaluate design concepts for specific joining applications of built-up attachments which could be used at rib-skin and spar-skin interfaces; second, to explore concepts for joining simple composite-composite and composite-metallic structural elements, identify the fundamental parameters controlling the static strength characteristics of such joints, and compile data for design, manufacture, and test of efficient structural joints using the Gr/PI material system. The major technical activities followed two paths concurrently. TASK 1 consisted of design allowables testing and design and test of specific built-up attachments. TASK 2 evaluated standard and advanced Gr/PI and Gr/PI to titanium bonded joints. An overall program flow for the two tasks is shown in Figure 2-1.

This document presents a summary of the test and analysis results of TASK 2, shown enclosed in a dashed box in Figure 2-1. The primary objectives were to provide data useful for evaluation of standard bonded joint concepts and design procedures, to provide the designer with increased confidence in the use of bonded high-performance composite structures, and to evaluate possible modifications to standard bonded joint concepts for improved efficiency.

This is one of five reports that fully document the results of activities performed under NASA contract NAS1-15644. The other four reports are:

1. Cushman, J. B.; and McCleskey, S. F.: Design Allowables Test Program, Celion 3000/PMR-15 and Celion 6000/PMR-15 Graphite/ Polyimide Composites, NASA CR 165840, 1982.

2. Cushman, J. B.; McCleskey, S. F.; and Ward, S. H.: Design, Fabrication and Test of Graphite/Polyimide Composite Joints and Attachments - Summary, NASA CR-3601, 1982.

3. Cushman, J. B.; McCleskey, S. F.; and Ward, S. H.: Design, Fabrication and Test of Graphite/Polyimide Composite Joints and Attachments - Data Report, NASA CR-165955, 1982.

4. Cushman, J. B.; McCleskey, S. F.; and Ward, S. H.: Test and Analysis of Graphite/Polyimide Bonded Joints - Data Report, NASA CR-165956, 1982.

Measurement Units

All measurement values in this report are expressed in the International System of Units and in U.S. Customary Units. Actual measurements and calculations were made in U.S. Customary Units.

4
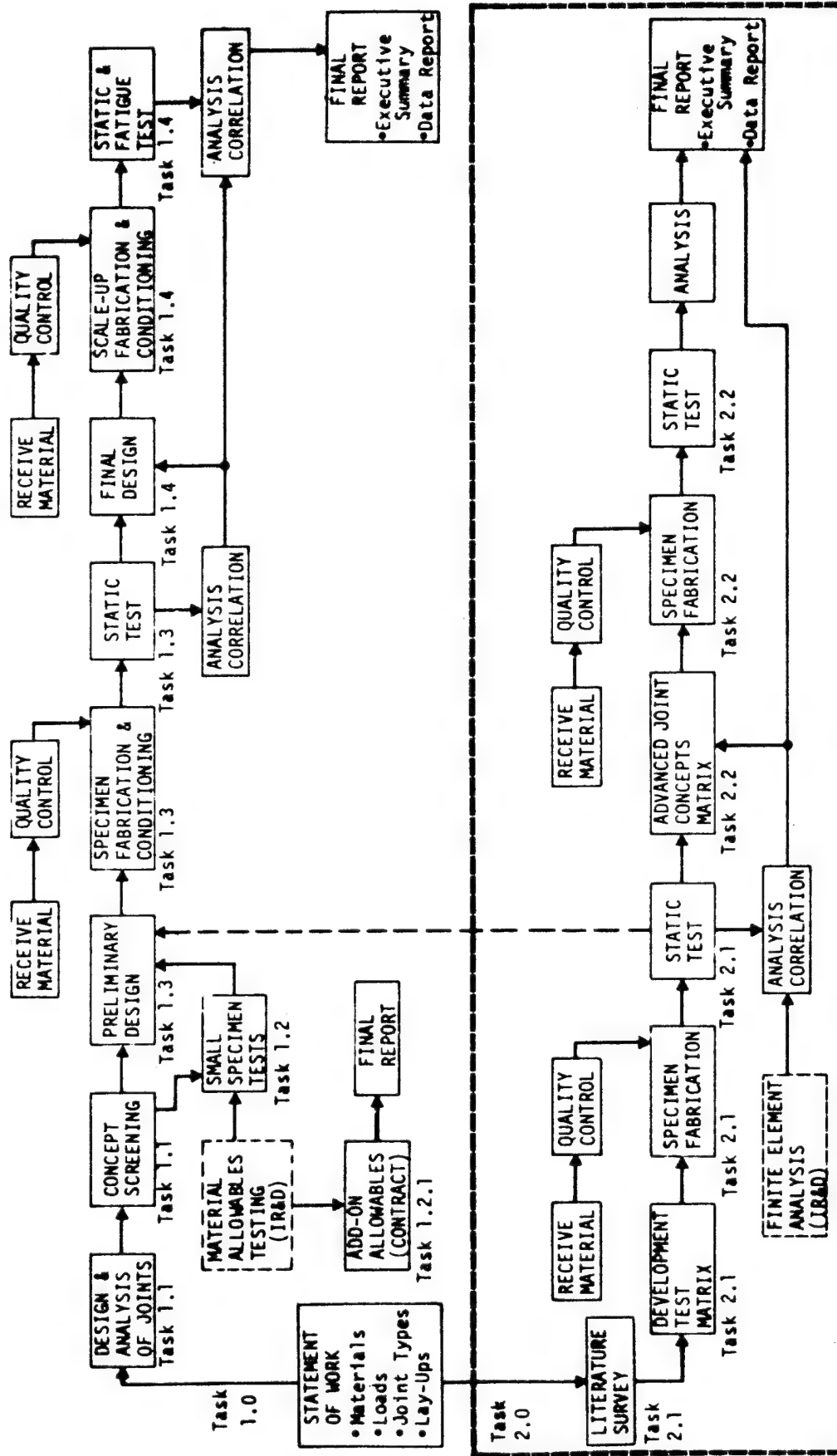
Figure 2-1: TASK 1 and TASK 2 PROGRAM FLOW

THIS PAGE INTENTIONALLY LEFT BLANK

3.0 LITERATURE SURVEY AND PERFORMANCE TRENDS

A literature survey was conducted to obtain information on graphite/polyimide composite design methods and joining parameters. Approximately 1500 articles and reports were identified as potentially relevant and based on the abstracts about 200 were selected for further study. Brief summaries of each report reviewed are reported in NASA Contract Report Numbers CR-159108 through CR-159115.

The following summary resulting from the literature search and finite element analyses (see Section 9.0) gives expected performance trends of bonded joints with respect to various parameters. Unless otherwise noted, these statements apply to both single- and double-lap joints:

o   Increasing the lap length increases joint strength towards an asymptote.

o   Increasing the axial and flexural stiffness of the adherends increases joint strength (because of reduced peel stresses).

o   Increasing the adherend thicknesses increases joint strength towards an asymptote.

o   Stiffness balanced joints are stronger than unbalanced joints (because of reduced peel stresses).

o   Tapering the ends of the adherends increases joint strength (because of reduced peel stresses).

o   Placing a "softer" ply group at the joint interface ($\pm 45^\circ$ vs. 0°) results in a more uniform shear strain along the joint interface, thus increasing double-lap joint strength.

o   Single-lap joints which have adherends with equal thermal expansion
     coefficients are stronger at 116K (-250°F) and 294K (70°F) than
     joints which have adherends that have thermal expansion imbalances.
     This is caused by increased moment and peel stresses in the
     adherend/adhesive resulting from the residual thermal stresses pre-
     sent in the joint. The effect of a thermal expansion imbalance is
     small at 561K (550°F) since this is close to the cure temperature
     (thermal stress free state).

o   Composite (Gr/PI) to metal (titanium) double-lap joints have a
     thermal expansion imbalance.   This suggests that these joints
     would not be as strong as an "all-composite" joint.   However,
     because the inner adherends are titanium and this is where the
     greatest peel stresses occur, these joints are stronger, since
     interlamina failures would occur in a composite inner adherend.

o   Increasing the temperature reduces residual stresses, softens the
     resin, and slightly reduces the strength of the composite adherend.
     The net result is an increase in joint strength with increasing
     temperature because of a reduction in severity of stress concentra-
     tions.   This assumes that the reduction in basic composite and
     adhesive material properties is small at the elevated temperature.

4.0 TEST PLAN DEVELOPMENT

The objective of the standard joint test program was to evaluate different types of bonded joints and the various parameters that affect static joint performance. Single-lap, double-lap and symmetric step-lap joints as shown in Figure 4-1 were selected as the joint types to be evaluated. Analyses of these joint types are common in the literature and they represent types commonly used in aerospace structures. Test matrices were established to evaluate joint strength parameters of temperature, lap length, adherend thickness, adherend axial stiffness, laminate stacking sequence and adherend tapering. The baseline laminate chosen was a quasi-isotropic layup to be consistent with Task 1.0 joints. Test matrices and specimen configurations are given in Tables 4-1 through 4-3. All specimens were conditioned at 589K (600°F) in a one atmosphere environment (air) for 125 hr. prior to test. A total of 186 single-lap joints, 258 double-lap joints, and 18 symmetric step-lap joints were tested. Test temperatures were 116K (-250°F), 294K (70°F) and 561K (550°F).

Based on results from the standard bonded joint testing, several advanced joint concepts were defined. These concepts and the corresponding test matrix are described in Section 8.0.

Gr/PI

Gr/PI or Titanium

SINGLE-LAP

Gr/PI

Gr/PI or Titanium

DOUBLE-LAP

Titanium

Gr/PI

SYMMETRIC STEP-LAP
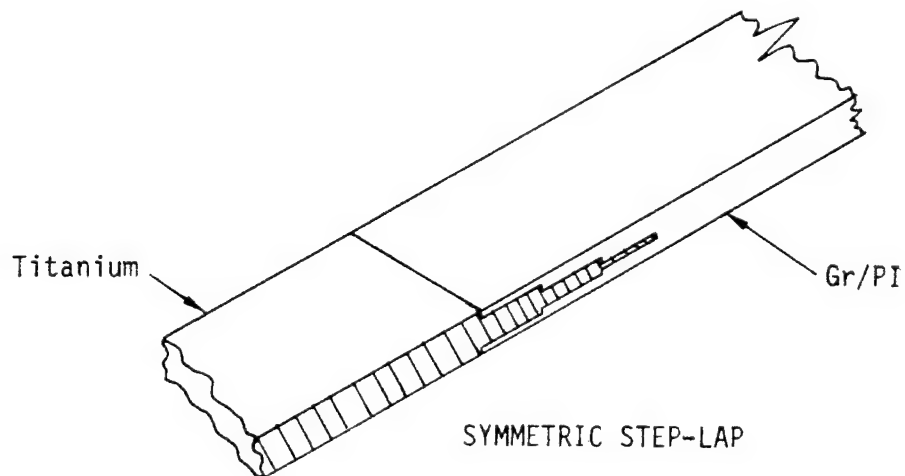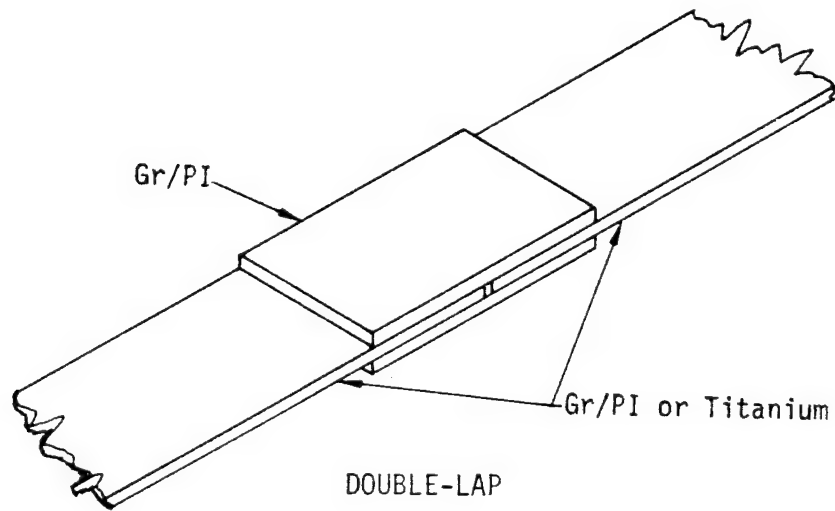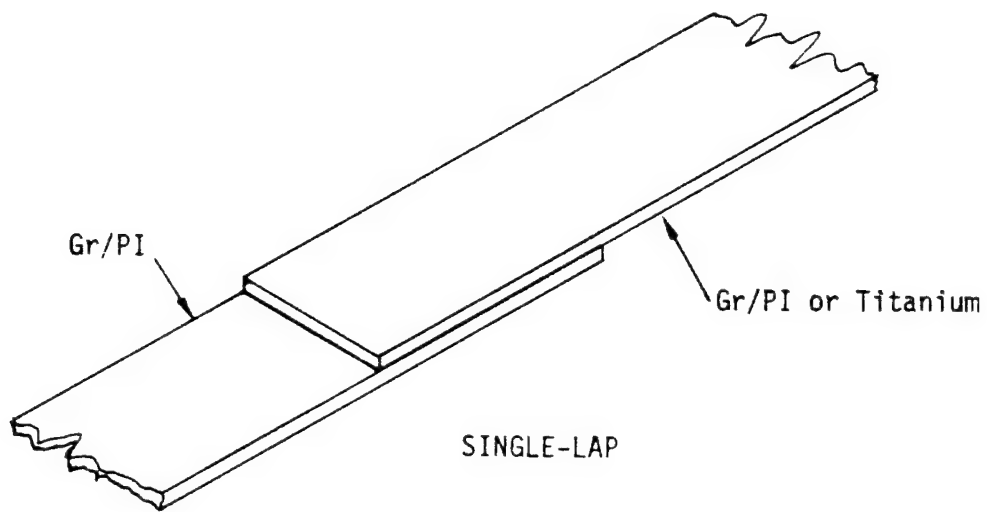
Figure 4-1: STANDARD BONDED JOINTS TESTED

Table 4-1: SINGLE LAP BONDED JOINT TEST MATRIX

Width = 25.4 mm (1.0 in.)

(Diagram labels: La, t, (Tapering))

Material	Configuration	LAP LENGTH (La) mm (in.)				ADHEREND THICKNESS (t) mm (in.)				ADHEREND LAYUP				TEMPERATURE K (°F)			NO. OF TESTS
		12.7 (.5)	25.4 (1.0)	50.8 (2.0)	75.2 (3.0)	Gr/PI 1.02/2.03 (.04/.08)	Gr/PI 1.52 (.06)	Gr/PI 2.54 (.10)	Ti .76 (.03)	$(0/\pm45/90)_{NS}$	$(0/\pm45/0_3)_{NS}$	$(\pm45/0/90)_{NS}$	$(0_3/\pm45_3/90_3)_{NS}$	116 (-250)	294 (70)	561 (550)	
Gr/PI – Gr/PI	BASELINE	●	●	●	●		●			●				●	●	●	72
	INCREASED ADHEREND STIFFNESS			●			●				●			●	●	●	18
	STACKING SEQUENCE			●			●					●			●		6
	STACKING SEQUENCE			●			●						●		●		6
	UNBALANCED ADHERENDS			●		●				●				●	●	●	18
	INCREASED THICKNESS			●				●		●					●		6
	TAPERED ADHERENDS			●				●		●					●		6
Gr/PI-Ti	BASELINE		●	●	●		●		●	●				●	●	●	54

TOTAL 186

11

Table 4-2: DOUBLE LAP BONDED JOINT TEST MATRIX

(Tapering) — La — t — 2t — Width = 25.4 mm (1.0 in.)

Material	Configuration	Lap Length (La) mm (in.)			Adherend Thickness (t) mm (in.)					Adherend Layup				Temperature K (°F)			No. of Tests
		20.3 (0.8)	33.0 (1.3)	45.7 (1.8)	Gr/PI 1.02 (.04)	Gr/PI 1.52 (.06)	Gr/PI 1.52/2.03 (.06/.08)	Gr/PI 3.05 (.12)	Ti 1.52 (.06)	$(0/\pm45/90)_{NS}$	$(0/45/0_2/-45/0)_{NS}$	$(0_3/\pm45_3/90_3)_{NS}$	$(\pm45/0/90)_{NS}$	116 (-250)	294 (70)	561 (550)	
Gr/PI – Gr/PI	BASELINE	•	•	•	•					•				•	•	•	54
	BASELINE	•	•	•		•				•				•	•	•	54
	INCREASED AXIAL STIFFNESS		•			•					•			•	•	•	18
	STACKING SEQUENCE		•			•						•		•	•	•	18
	STACKING SEQUENCE		•			•							•	•	•	•	18
	UNBALANCED ADHERENDS		•				•			•				•	•	•	18
	INCREASED THICKNESS		•					•		•					•	•	12
	TAPERED ADHERENDS		•					•		•					•	•	12
Gr/PI – Ti	BASELINE		•	•					•	•				•	•	•	36
	STACKING SEQUENCE			•					•				•	•	•	•	18

TOTAL 258

12

Table 4-3: SYMMETRIC STEP LAP BONDED JOINT TEST MATRIX

4.06 mm (.16 in.)   Width = 25.4 mm (1.0 in.)
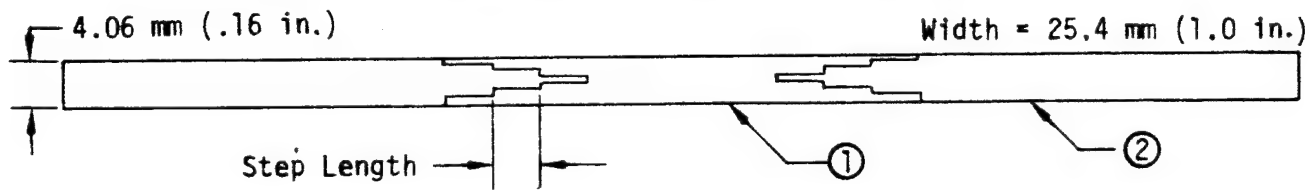
Step Length

| CONFIGURATION | STEP LENGTH | | NUMBER OF TESTS | MATERIAL | |
	mm	(in.)		①	②
3-Step	13	(.51)	18	Graphite/Polyimide (0/±45/90)$_{NS}$	Titanium-6Al-4V

THIS PAGE INTENTIONALLY LEFT BLANK

5.0 MATERIALS AND SPECIMEN FABRICATION

Following are brief descriptions of the principal materials used in this program along with laminate processing and specimen fabrication procedures. Typical mechanical properties are listed in Table 5-1.

Composites

Composite joints characterized under this program were made from graphite/polyimide tape materials. Based on previous experience from the CASTS* program research, Boeing and NASA chose the Celion/PMR-15 material system. The graphite fiber was Celion 3000, with NR150B2G polyimide sizing. Preimpregnated tape was procured from US Polymeric, Inc. to a material specification contained in Reference 1. Gr/PI and S-glass/PI fabric used in the "advanced" joint test matrix were preimpregnated in the Boeing Materials Technology labs. Laminates were processed according to procedures developed under NASA Contract NAS1-15009.

Adhesive

The high-temperature adhesive utilized is designated A7F. A7F is a 50:50 resin solids copolymer blend of LARC-13 adhesive (supplied by NASA, Langley) (Ref. 2) and AMOCO's AI-1130 Amide-Imide. Sixty percent by weight aluminum powder and 5% by weight Cab-O-Sil are added. The adhesive was applied to 112 E-glass scrim to form a .25mm (.01 in.) thick adhesive film.

Titanium

The titanium used was Ti-6Al-4V (standard) per MIL-T-9046, Type III, Composition C.

*Composites for Advanced Space Transportation Systems (Contracts NAS1-15009 and NAS1-15644).

15

Specimen Fabrication - Bonded Joint Tests

All test specimens were fabricated in the Boeing Materials Technology laboratories using the procedure flow shown in Figure 5-1. Quality control tests were conducted on all lots of prepreg to verify flexural modulus and strength and interlaminar shear strength prior to specimen fabrication.

Chemical characterization tests of the resin were conducted using high pressure liquid chromatography, mass spectroscopy, infrared spectroscopy, and thermal gravimetric analysis.

Celion 3000/PMR-15 laminates were fabricated using processing procedures defined in Reference 1.

Joints were bonded using A7F adhesive film. All titanium surfaces were chromic-acid anodized and primed with A7F primer. After joint bonding and conditioning, the bond lines were C-scanned to determine acceptability. Adhesive film was not used for symmetric step lap joints. The prepreg was layed-up on the steps and the joint was co-cured as an assembly.

Specimen Fabrication-Adhesive Tests

Specimens for the adhesive tests were prepared using standard laboratory practices. Titanium surfaces were chromic-acid anodized and primed with A7F primer. Specimen were assembled using the A7F adhesive film and cured using the procedures in Reference 1.

16

Table 5-1: TYPICAL ROOM TEMPERATURE MATERIAL PROPERTIES

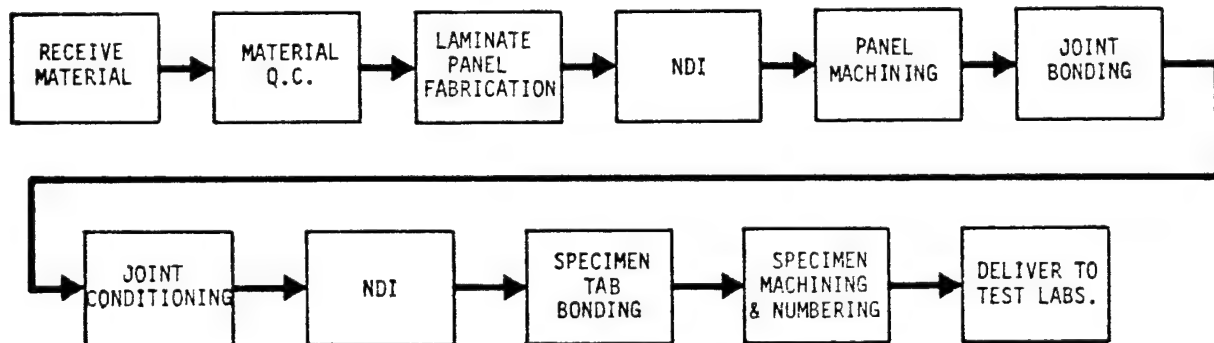| MATERIAL	F_{tu}		E_T	F_{su}		G_{xy}		CTE cm/cm-K
	MPa	(ksi)	GPa(10^6Psi)	MPa	(ksi)	MPa	(ksi)	(in/in^{o}F)
CELION 3000/PMR-15* (51.4% FV)								
0°	1289	(187)	130 (18.8)	——		——		——
90°	45	(6.6)	8.3 (1.2)	——		——		
(0/$\pm$45/90)$_{4S}$	476	(69)	50.3 (7.3)	——		——		2.7 (1.5)$\times10^{-6}$
ADHESIVE* A7F	——		——	16	(2.3)	80	(11.6)	17.5 (9.7)
TITANIUM 6Al-4V	924	(134)	110 (16)	544	(79)	43	(6.2)	9.7 (5.4)

* Aged 125 hr at 589K (600°F)

Figure 5-1: BONDED JOINT FABRICATION FLOW

THIS PAGE INTENTIONALLY LEFT BLANK

6.0 ADHESIVE CHARACTERIZATION

To support design and analysis of bonded joints it was necessary to character-
ize the adhesive system. The adhesive is designated A7F (LARC-13 Amide-Imide
modified) and is described in section 5.0. The A7F adhesive test matrix is
shown in Table 6-1. Specimen configurations are shown in Figures 6-1 through
6-3. Tests were conducted in the Boeing materials test laboratories to
measure average shear strength, and flatwise tension strength. Special
"thick adherend" shear tests were conducted under subcontract by Dr. J. R.
Vinson at the University of Delaware. These tests measured ultimate shear
strength, shear modulus and ultimate shear strain. All test specimens were
fabricated by Boeing. Coefficient of thermal expansion (CTE) tests were
conducted during the design allowables testing under TASK 1.2.1 (Ref. 3);
however, results are included here for completeness.

Adhesive Test Results

Average test results for the 12.7 mm (0.5 in.) single lap shear, "thick
adherend" shear and flatwise tension tests are shown in Table 6-2 for the
various conditionings and test temperatures.

Since the "thick adherend" test specimen has lower peel stresses than the
standard single lap specimens, it was expected that the shear strengths from
this test would be higher than those from the titanium lap shear (ASTM D 1002)
tests. Results for cured/post-cured specimens at 294K (70°F) and 561K (550°F)
are higher for the ASTM D 1002 procedure than for the "thick adherend"
procedure. ASTM D 1002 results for aged specimens were slightly higher than
"thick adherend" results at 561K (550°F).

There is no known explanation for these anomalies other than possible material
and processing variations. C-scans of the bond lines showed no defects.
Adhesive thicknesses could have been different for the two specimen configu-
rations. Also there may have been some edge effects during the curing or
aging. The thick adherend specimens were conditioned as a single plate

approximately 508 mm (20 in.) wide and then cut into specimens. The ASTM D 1002 specimens were made from standard titanium "finger" blanks 25.4 mm (1.0 in.) wide which may have contributed to edge effects.

The average shear modulus from the "thick adherend" tests was 58 MPa (8000 psi) with the data showing drops in moduli at both cryogenic and elevated temperature with respect to room temperature. The room temperature aged specimens exhibited a bimodulus behavior. Results from the same tests show a decrease in ultimate shear strain with increasing temperature.

Flatwise (out-of-plane) tension tests were conducted on cured/post-cured specimens that had stainless steel bars, while the aged specimens had titanium bars. All specimens failed cohesively. Test results show a drop in strength with an increase in temperature. On the average, flatwise tension strength for A7F adhesive are twice that for a Celion 3000/PMR-15 laminate (Ref. 3). This indicates that joints with strengths governed by peel failures will fail in the laminate rather than in the adhesive.

Results of coefficient of thermal expansion (CTE) tests on A7F adhesive conducted under contract TASK 1.2.1 are shown in Figure 6-4. Data show a significant drop in CTE due to aging.

Conclusions

Results of the adhesive testing shows that A7F maintains a shear strength greater than 8.3 MPa (1200 psi) in the temperature range of 116K (-250°F) to 589K (550°F). It maintains this strength after exposure to environmental conditions of aging and thermal cycling. A7F maintains a flatwise tension strength above 11.0MPa (1600 psi) at 561K (550°F) with significant increases in strength with decreased temperature. CTE data for the A7F adhesive show a significant drop due to aging.

20

Table 6-1: TEST MATRIX 2 - A7F
### (LARC-13 Amide-Imide Modified) ADHESIVE

TEST		CONDITIONING ▷	NUMBER OF TESTS AT			TOTAL NUMBER OF TESTS	TEST PROCEDURES	SPECIMEN CONFIGURATION
NO.	TYPE		116K (-250"F)	RT	561K (550"F)			
3	SHEAR	1 2 3	3 3 3	3 3 3	3 3 3	9 9 9	ASTM D1002	FIGURE 6-1
4	SHEAR	1 2	3 3	3 3	3 3	9 9	U of D* Thick Adherend	FIGURE 6-2
5	TENSION	1 2	3 3	3 3	3 3	9 9	ASTM D2095	FIGURE 6-3

▷ CONDITION CODE   *U of D - University of Delaware

1 - As cured/postcured

2 - Soaked for 125 hours at 589K (600°F) in a one (1) atmosphere environment (air)

3 - Thermally cycled 125 times in a temperature range from 116K to 589K (-250°F to 600°F) and in a one (1) atmosphere environment (air)
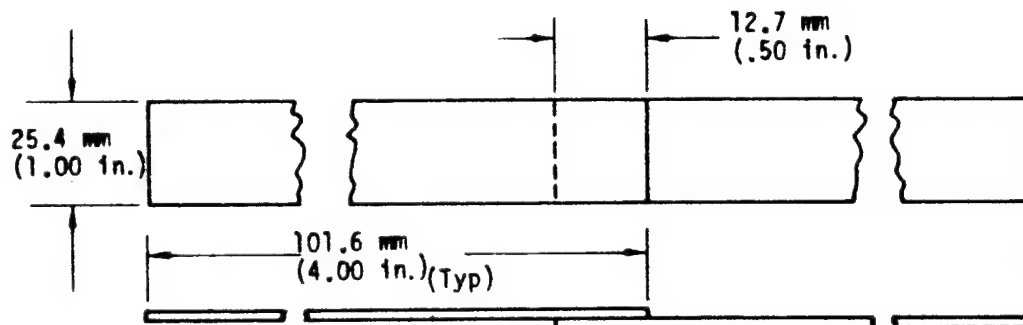
MATERIAL: TITANIUM 6A1-4V ANNEALED
1.07 mm (.042 in.) NOM.
BOND WITH LARC-13 (A7F)
.254 mm (.01 in.) THICK

(ASTM D1002 STANDARD)

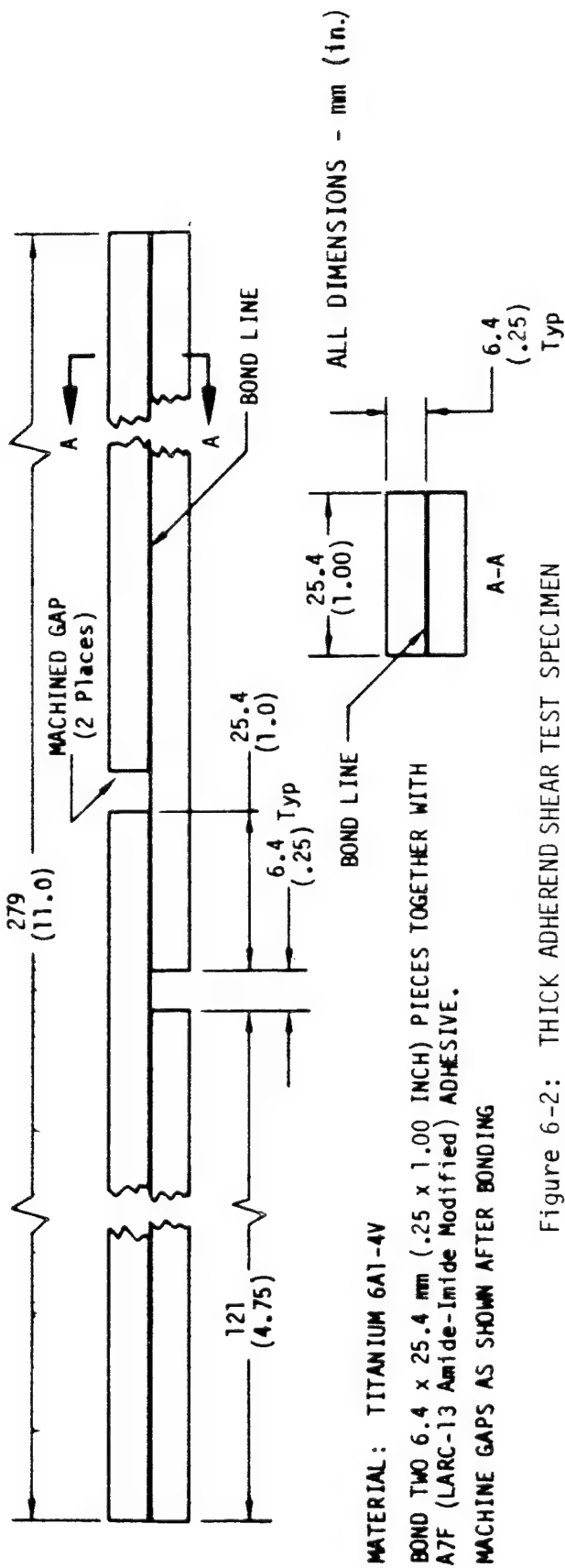Figure 6-1:   TITANIUM SINGLE LAP SHEAR SPECIMEN

ALL DIMENSIONS - mm (in.)

MACHINED GAP
(2 Places)

BOND LINE

279
(11.0)

121
(4.75)

25.4
(1.0)

6.4
(.25) Typ

25.4
(1.00)

6.4
(.25)
Typ

BOND LINE

A-A

MATERIAL: TITANIUM 6A1-4V

BOND TWO 6.4 x 25.4 mm (.25 x 1.00 INCH) PIECES TOGETHER WITH
A7F (LARC-13 Amide-Imide Modified) ADHESIVE.

MACHINE GAPS AS SHOWN AFTER BONDING

Figure 6-2: THICK ADHEREND SHEAR TEST SPECIMEN

31.8 mm
(1.25 in.) Dia.

38.1 mm
(1.50 in.)

BONDED WITH A7F
.254 mm (.01 in.)
THICK ADHESIVE
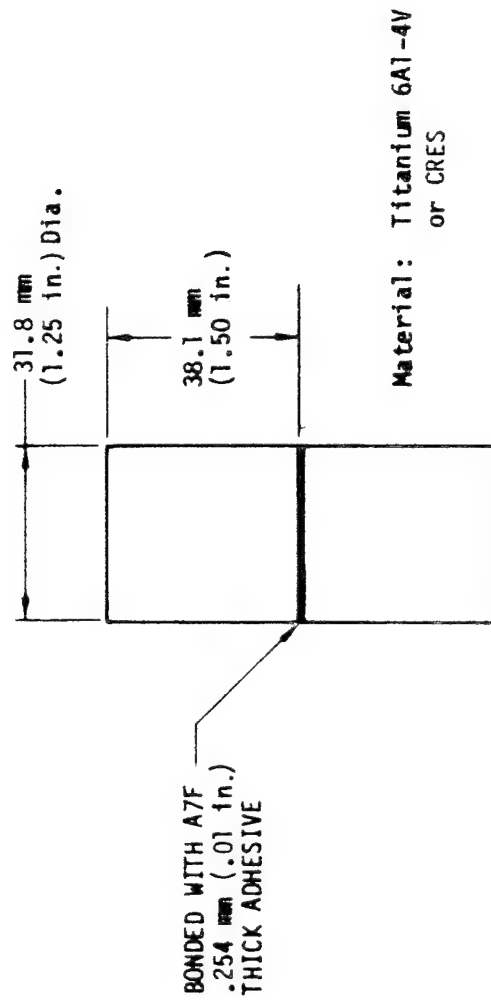
Material: Titanium 6A1-4V
or CRES

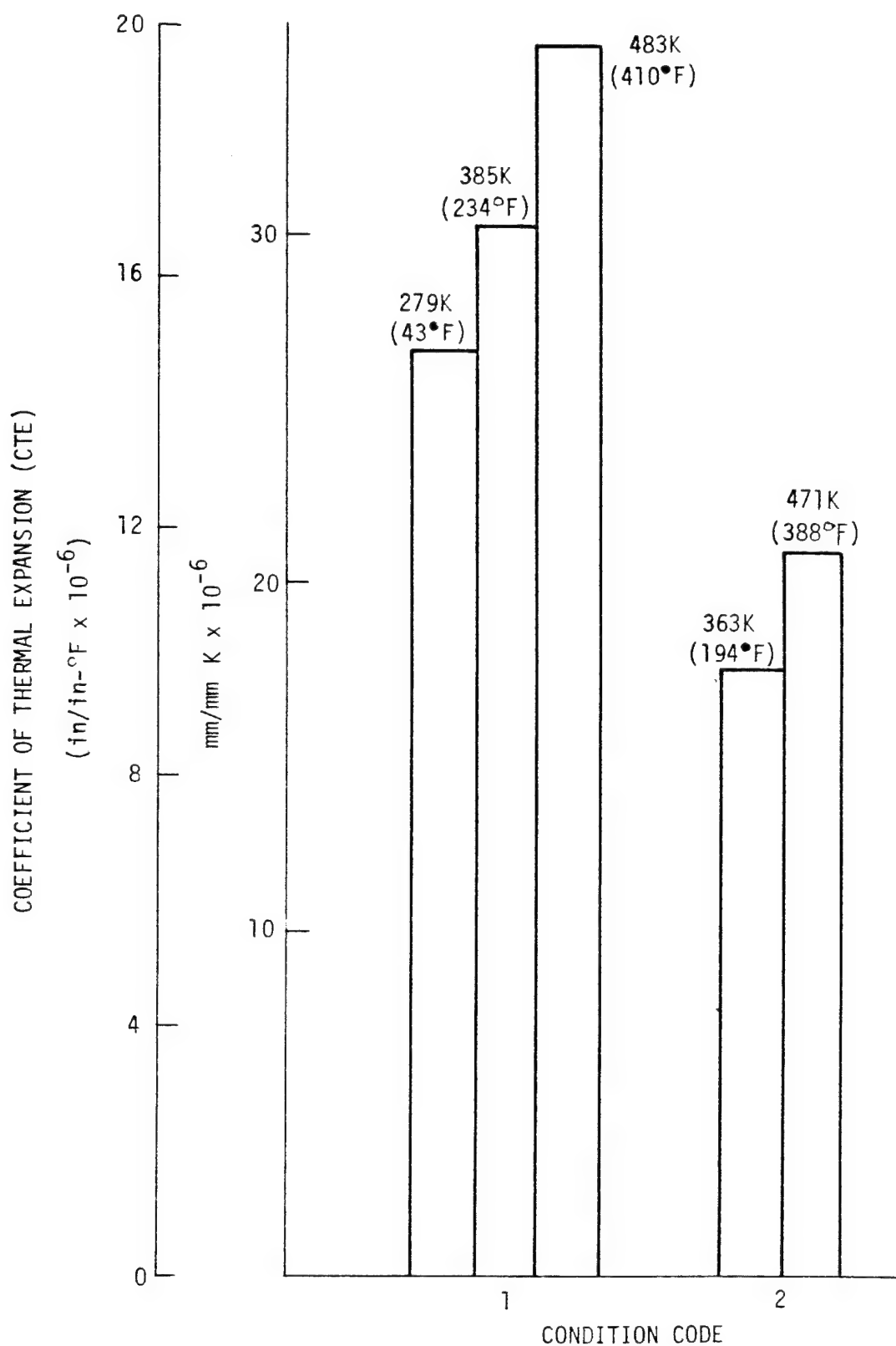Figure 6-3: FLATWISE TENSION ADHESIVE TEST SPECIMEN

22

Table 6-2: AVERAGE TEST RESULTS FOR A7F ADHESIVE

(a) SI Units

CONDITIONING	TEMPERATURE K	LAP SHEAR ASTM D 1002 SHEAR STRENGTH MPa	"THICK ADHEREND" TESTS			FLATWISE TENSION STRENGTH MPa
			SHEAR STRENGTH MPa	SHEAR MODULUS MPa	SHEAR STRAIN	
Cured/ Post Cured	116	20.7	22.57	61.83	.7085	55.01
	294	19.67	16.72	70.37	.4000	22.58
	561	13.53	8.79	45.82	.4276	11.65
Aged 125 hrs @ 589K (600°F)	116	14.75	21.21	40.72	.6305	45.15
	294	14.11	16.09	79.92 Init. 53.53 Sec.	.5263	27.37
	561	14.34	13.33	52.70	.4459	22.10
Cycled 125 Times -116K (-250°F to 589K (600°F)	116	11.56	—	—	—	—
	294	12.18	—	—	—	—
	561	15.63	—	—	—	—

(b) US Customary Units

CONDITIONING	TEMPERATURE F	LAP SHEAR ASTM D1002 SHEAR STRENGTH psi	"THICK ADHEREND" TESTS			FLATWISE TENSION STRENGTH psi
			SHEAR STRENGTH psi	SHEAR MODULUS psi	SHEAR STRAIN	
Cured/ Post-Cured	-250	3003	3274	8968	.7085	7978
	70	2853	2425	10206	.4000	3273
	550	1963	1275	6645	.4276	1690
Aged 125 hrs @ 589K (600°F)	-250	2140	3076	5906	.6305	6549
	70	2047	2333	11592 Init. 7764 Sec.	.5263	3970
	550	2080	1933	7643	.4459	3205
Cycled 125 Times - 116K (-250°F) to 589K (600°F)	-250	1676	—	—	—	—
	70	1767	—	—	—	—
	550	2180	—	—	—	—

Figure 6-4: COEFFICIENT OF THERMAL EXPANSION-- "A7F" ADHESIVE

7.0 STANDARD BONDED JOINTS

7.1 Standard Joint Test Results

Test results obtained for the single- and double-lap joints had a significant amount of data scatter. Coefficients of variation ranged from 0.023 to 0.410. Normally, large scatter can be attributed to processing and manufacturing variables. However, since all laminate adherends received strict process control, no conclusive explanation was found for the data scatter. Therefore, comparisons between joint types and analysis/correlations are based on average failure loads only. It is possible that the large data scatter may have masked the effect of parameter changes and thus affected the conclusions drawn from the test results.

In most cases the "Gr/PI-Gr/PI" joints exhibited an intralamina failure mode caused by peel stresses in the composite adherends as shown in Figure 7-1. This failure mode consists of a failure within a ply, as opposed to an interlamina mode where the failure occurs between plies. For both single- and double-lap joints, the intralamina failure occured in the ply nearest the joint interface, with the failure occurring for the double-lap joint in the inner adherends.

The "Gr/PI-titanium" specimens also exhibited intralamina and/or interlamina failures in the plies near the joint interface; however, some specimens also had adhesive failures over a portion of the joint. Evidence of partial adhesive failure occurred at all test temperatures but was predominant at the elevated temperature.

Figures 7-2 through 7-7 are comparisons of single- and double-lap joints. Failure loads versus lap length for single- and double-lap "Gr/PI-Gr/PI" and "Gr/PI-titanium" joints are shown in Figures 7-2 and 7-3 respectively. As expected there was a general increase in failure load with increasing lap length, with the loads appearing to approach asymptotes. Figures 7-4 and 7-5 show failure loads versus weight increment, defined in Figure 7-6, for

"Gr/PI-Gr/PI" and "Gr/PI-titanium" joints respectively. These curves show that a point is reached where adding more weight (increasing the lap length) does not result in an increase in strength.

Joint analysis indicates that double-lap joints should be more structurally efficient. Joint efficiency is defined as the average failure load divided by the adherend ultimate load. Joint efficiencies of "Gr/PI-Gr/PI" single-lap joints varied from 0.10 to 0.27 and for double-lap joints from 0.18 to 0.42. Efficiencies of "Gr/PI-titanium" single-lap joints ranged from 0.14 to 0.38 and for double-lap joints from 0.24 to 0.62. The greater efficiency of double-lap joints results from elimination of the load eccentricity and corresponding moment that is present in unsupported single-lap joints.

Figure 7-7 shows average weight coefficient (defined in Figure 7-6) versus lap length for single- and double-lap "Gr/PI-Gr/PI" joints. These curves indicate that for the same lap length, the single- and double-lap joints are approximately equal in load carried per unit weight of joint. Thus the double-lap joints, which have joint efficiencies approximately twice that of single-lap joints, are not more weight efficient than the corresponding single-lap joints.

Results for the "3-step" symmetric step-lap joints are shown in Figure 7-8. As was expected there is a strong temperature dependence in the strength of these joints. This is attributable to the difference in coefficients of thermal expansion between the Gr/PI and titanium adherends and the elevated cure temperature, which result in residual thermal stresses in the joint and thus decreased strength at lower temperatures.

A comparison of "Gr/PI-titanium" double lap joints with the "3-step" symmetric step-lap joint shows them to be about equal in strength for the lap lengths tested. At these load levels a double-lap joint would be the better design solution because of simplicity in manufacturing (other design constraints such as fatigue resistance, surface smoothness or weight may not allow this). Higher loads would dictate a symmetric step-lap (with more than

3 steps) or a scarf joint since increasing the lap length of a double-lap joint would not result in any significant additional strength.

Effects of changes in the various joint parameters tested are summarized in Table 7-1. Given are the percent changes in joint failure loads with respect to the appropriate baseline configuration. Baseline joints were those with $(0/\pm45/90)_{NS}$ layups and the same lap length and thickness. The table indicates that increased adherend stiffness, tapered adherends and a $(\pm45/0/90)$ layup are all viable methods for improving the strengh of both single and double lap joints.

In general, failure loads for the standard joints increased with increasing temperature, with the change in loads from cryogenic to room temperature being less than the change in loads from room to elevated temperature. For the "Gr/PI-Gr/PI" joints the average change in failure load from room to cryogenic temperature was -1% (values ranged from -36% to +10%), while the average change from room to elevated temperature was 24% (values ranged from -6% to 85%). In contrast, the effect of temperature on the "Gr/PI-titanium" joints was more pronounced due to the thermal expansion imbalance in the joint. The average change in failure load from room to cryogenic temperature was -23% (values ranged from -6% to -38%), while the average change from room to elevated temperature was 47% (values ranged from -4% to 93%). The large data scatter precludes drawing conclusions about the effect of the various joint parameters on the temperature dependence of bonded joints, other than that a thermal expansion imbalance in the joint increases the temperature dependence. However, it appears from Table 7-1 that the beneficial effects of increased adherend stiffness, tapered adherends, etc. are much greater at 561K (550°F) than at room or cryogenic temperatures.

The maximum joint loads achieved in the standard joint test program are summarized in Figure 7-9. The maximum load achieved for a single-lap joint (25.4 mm (1.0 in.) wide) was 9.71 kN (2184 lb) while for the double-lap and step-lap joints (25.4 mm (1.0 in.) wide) it was 24.64 kN (5540 lb) and 22.89 kN (5147 lb) respectively. All three maximums occurred at a test temperature of

561K (550°F). Maximum loads shown should not be construed to be the maximum obtainable. Other layups or joint configurations for a particular joint type could have resulted in higher failure loads.

7.2 Standard Joint Conclusions

Results of the standard joints testing have demonstrated that Gr/PI bonded joints will carry loads of the magnitude expected for advanced aerospace vehicles at temperatures from 116K (-250°F) to 561K (550°F). Adherend tapering and careful selection of adherend stiffness and lamina stacking can result in significant improvement in joint efficiency. The failure loads of Gr/PI bonded joints show a significant temperature dependence. In general, failure loads increase with increasing temperature, with a stronger dependence shown by the "Gr/PI-titanium" joints than the "Gr/PI-Gr/PI" joints. The weak link in joint strength was the low transverse tension strength of the composite. Modifications to the material system that would result in an increase in that property or changes in the joint design that reduce or eliminate peel stresses would provide a significant increase in overall joint performance for all standard joint types.

See Detail Below ⟶

SINGLE-LAP JOINT

See Detail Below

DOUBLE-LAP JOINT

Lamina ⟶

Intralamina Failure
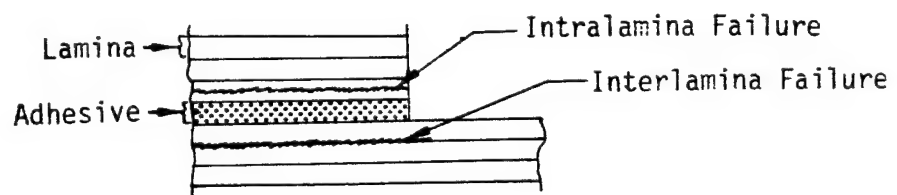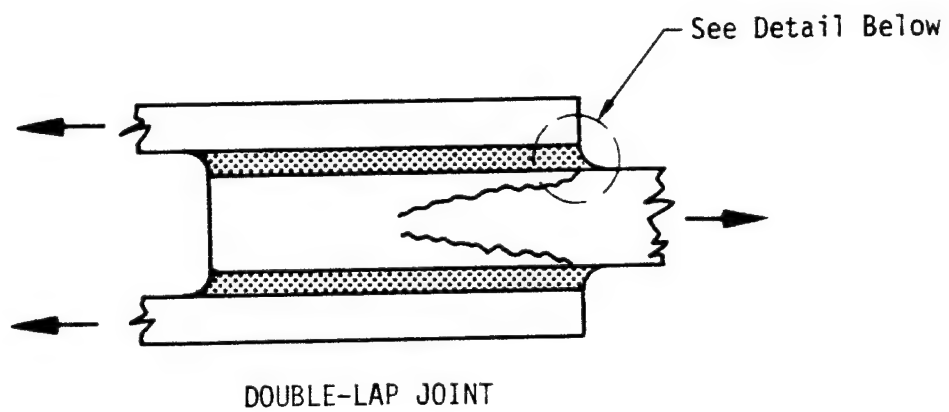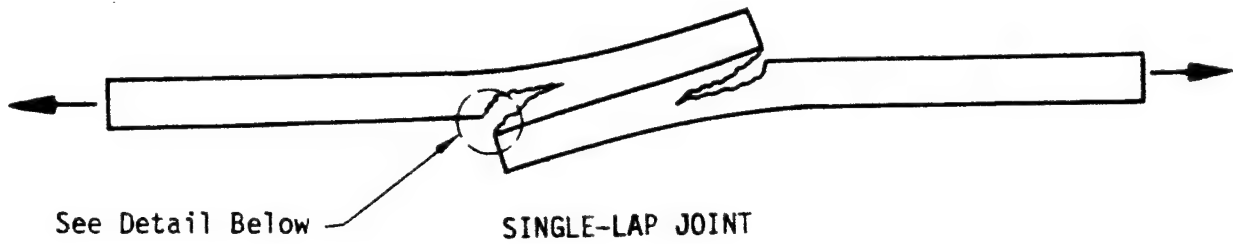
Interlamina Failure

Adhesive ⟶

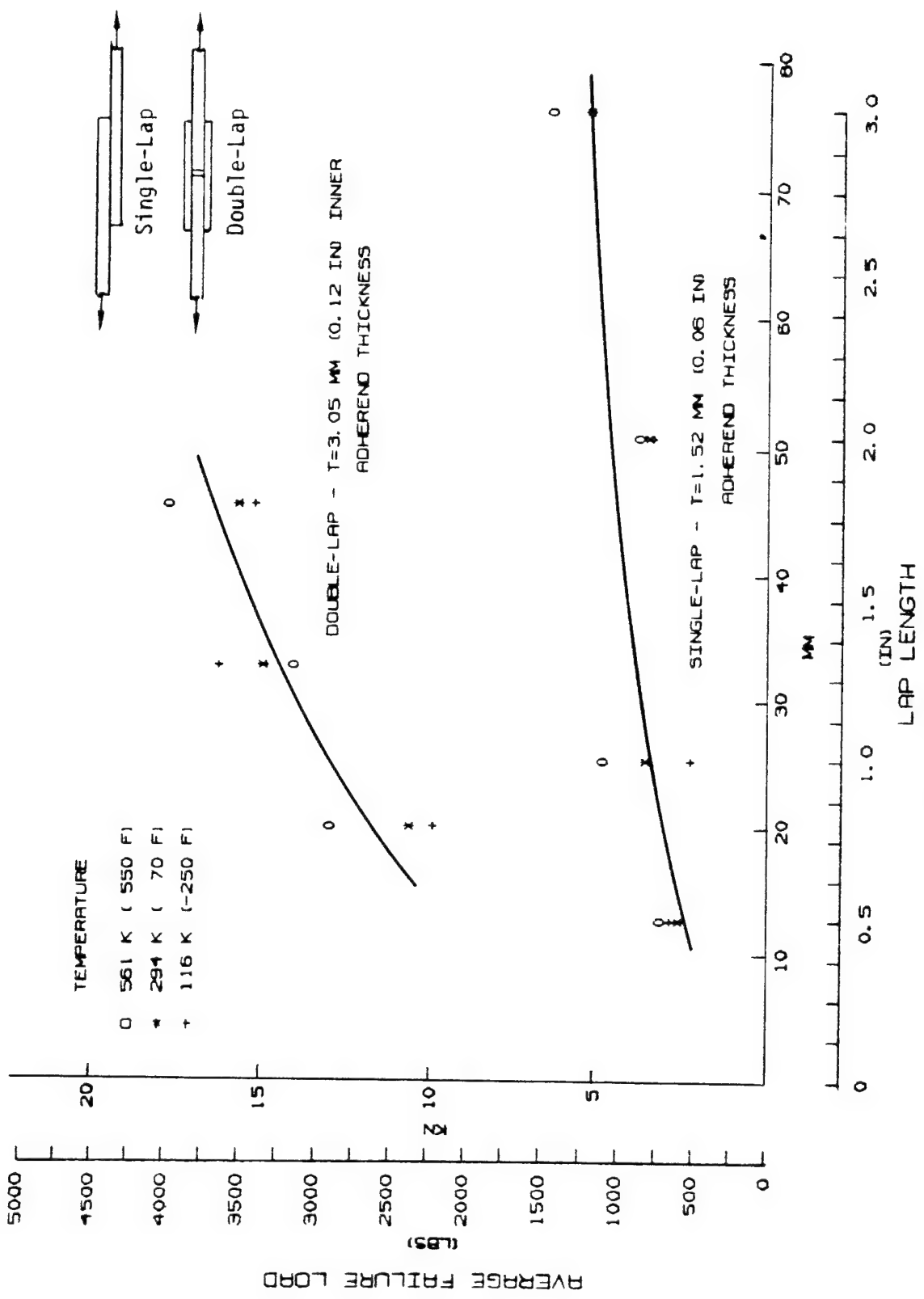Figure 7-1: PEEL FAILURES OF COMPOSITE BONDED JOINTS

Figure 7-2: COMPARISON OF SINGLE- AND DOUBLE-LAP JOINTS
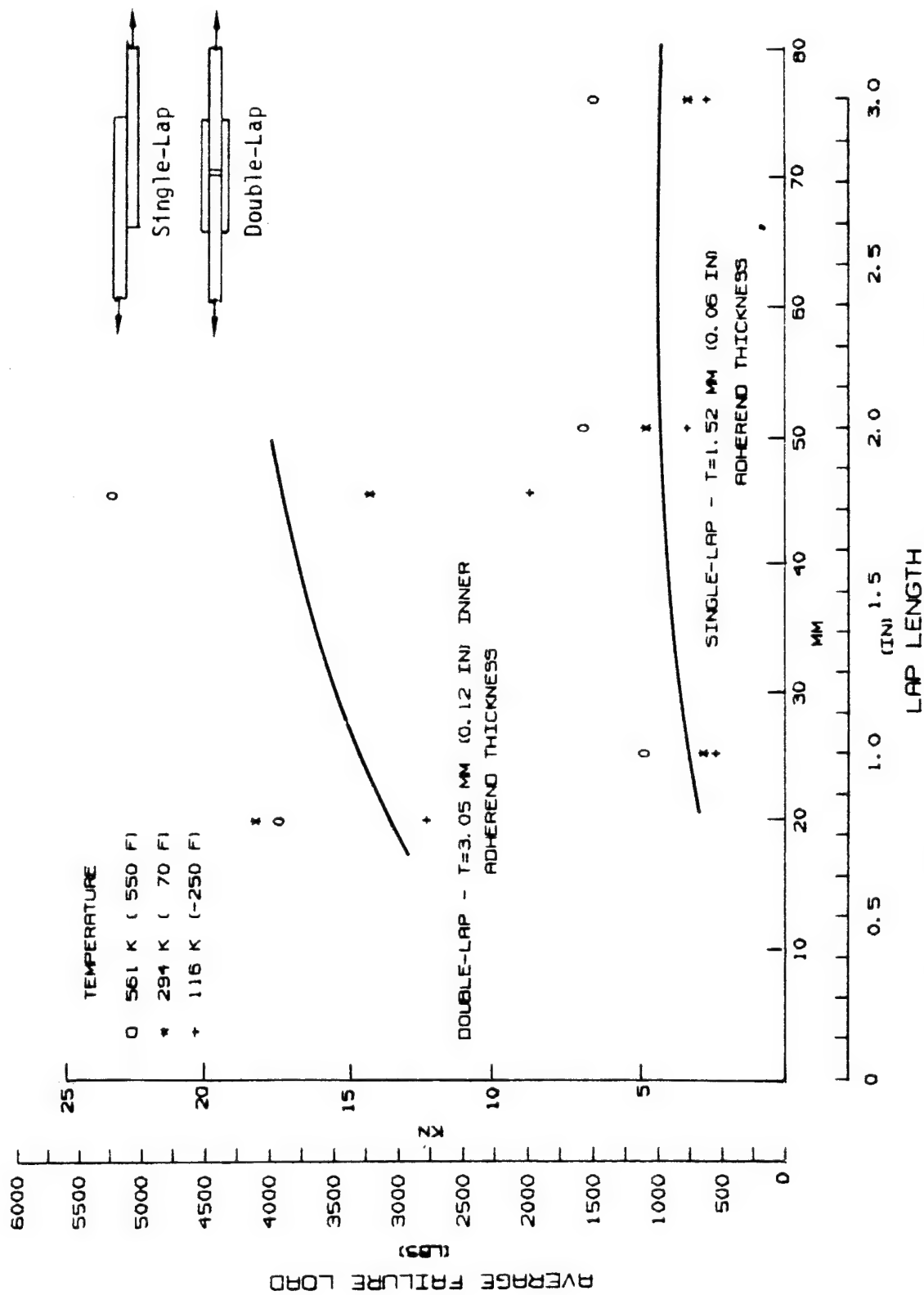GR/PI TO GR/PI JOINTS

Figure 7-3: COMPARISON OF SINGLE- AND DOUBLE-LAP JOINTS
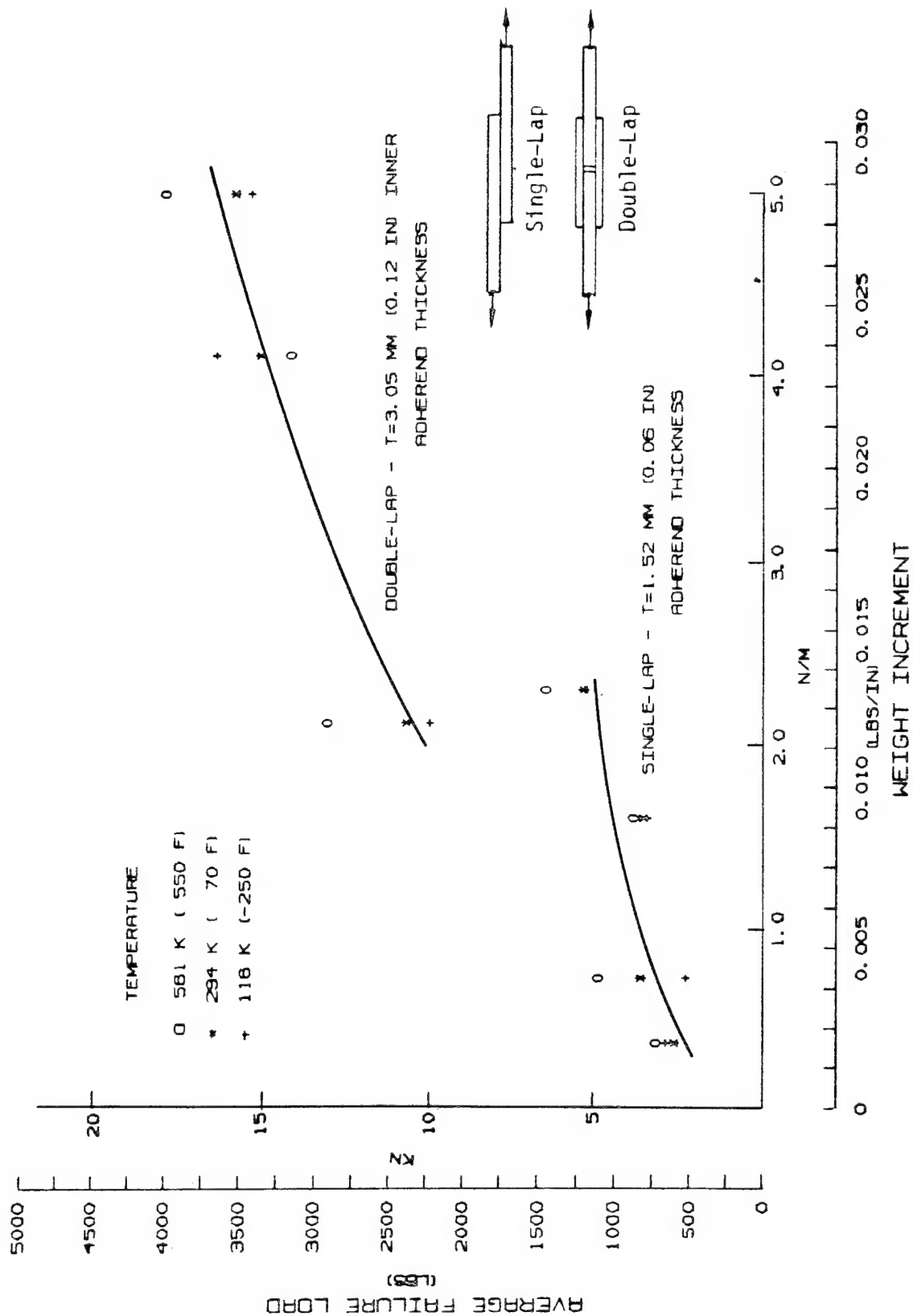GR/PI TO TITANIUM JOINTS

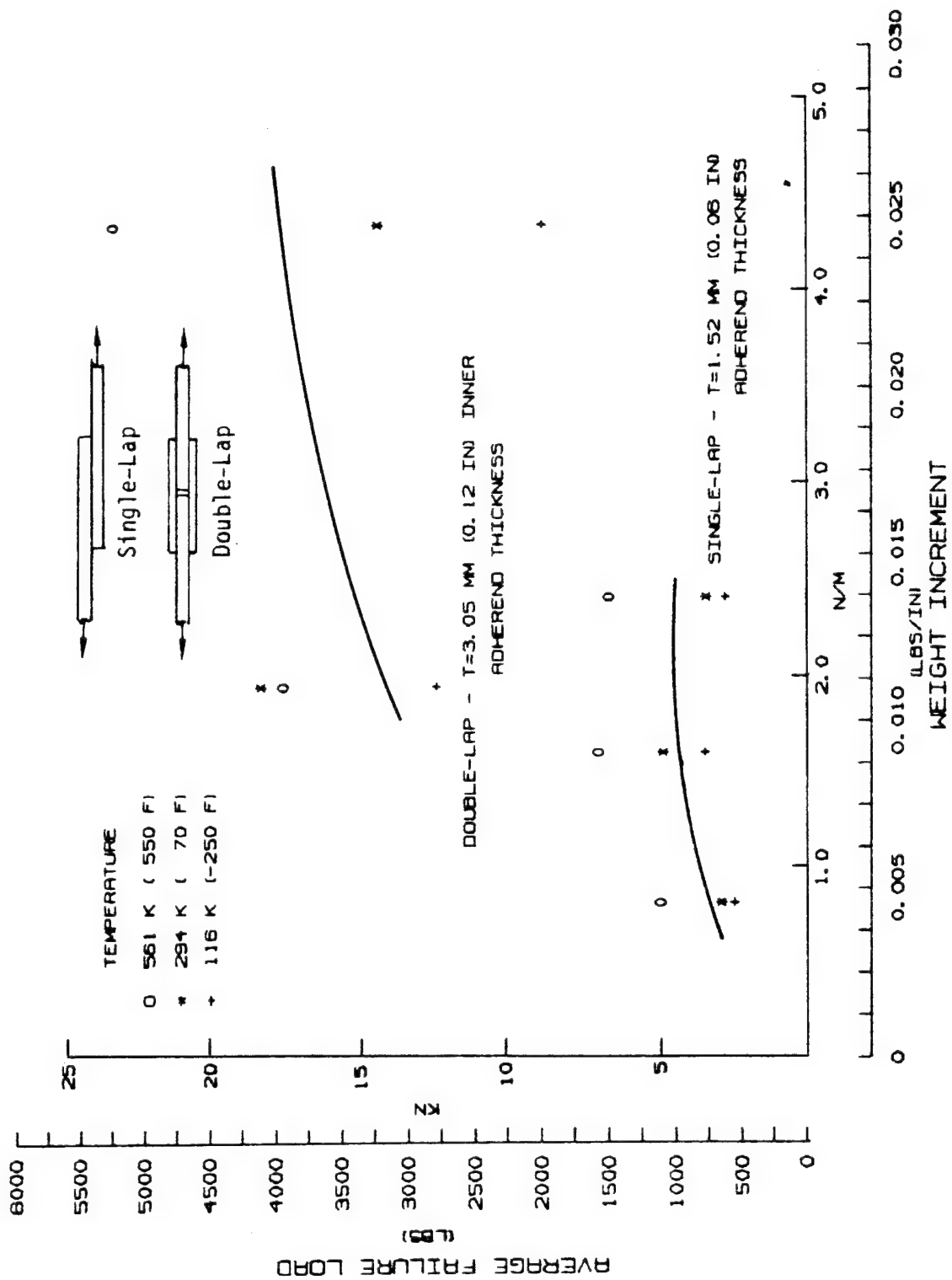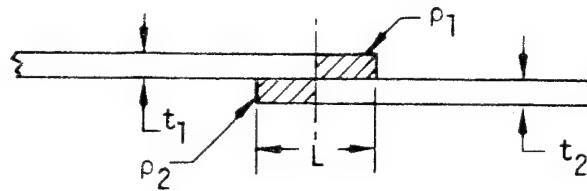Figure 7-4: COMPARISON OF SINGLE- AND DOUBLE-LAP JOINTS GR/PI TO GR/PI JOINTS

32

Figure 7-5: COMPARISON OF SINGLE- AND DOUBLE-LAP JOINTS GR/PI TO TITANIUM JOINTS
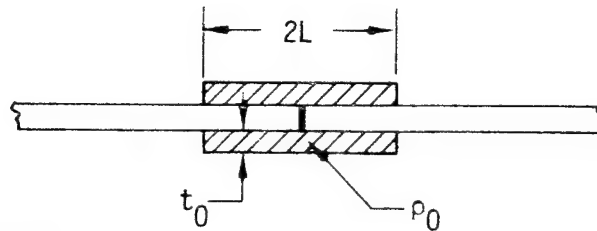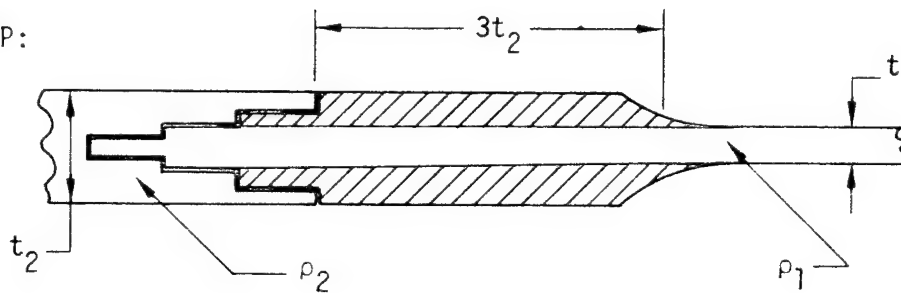
33

WEIGHT INCREMENT (ΔW)

SINGLE-LAP:

$$\Delta W = \frac{1}{2}L \; (\rho_1 t_1 + \rho_2 t_2)$$

DOUBLE-LAP:

$$\Delta W = 2 \cdot 2L \cdot t_0 \; \rho_0 = 4L t_0 \rho_0$$

STEP-LAP:

$$t_1 = \frac{F_2^{TU}}{F_1^{TU}} \, t_2$$

F_i^{TU} = Ultimate Tensile Strength of Material i

ρ = Density

$$\Delta W \approx \rho_1 3 t_2 (t_2 - t_1)$$

$$\Delta W \approx 3 \rho_1 t_2^2 \; (1 - F_2^{TU}/F_1^{TU})$$

$$\text{AVERAGE WEIGHT COEFFICIENT} = \frac{\text{AVERAGE FAILURE LOAD}}{\text{WEIGHT INCREMENT}} = \frac{P}{\Delta W}$$

Figure 7-6: CALCULATION OF WEIGHT INCREMENT & AVERAGE WEIGHT COEFFICIENT
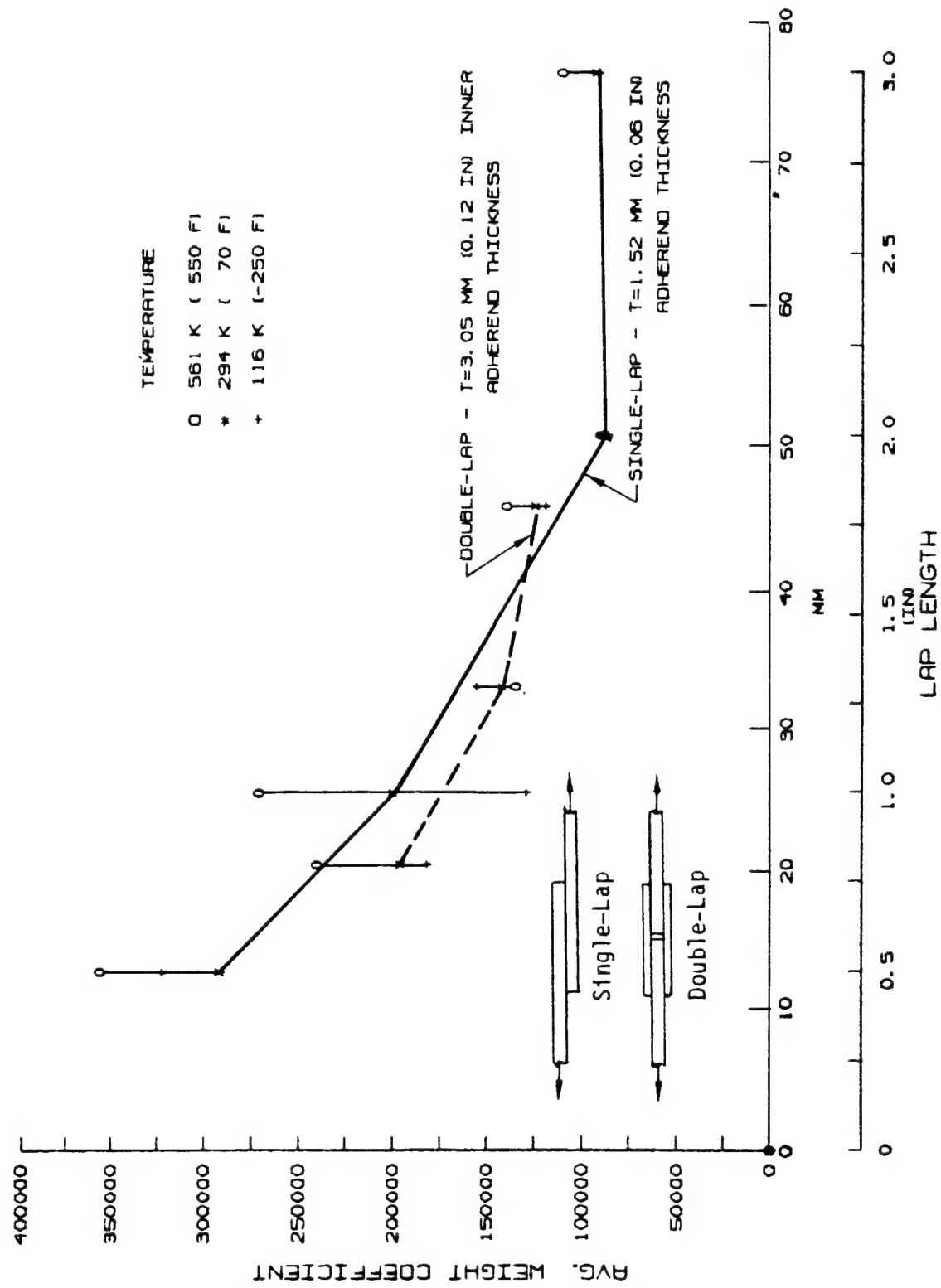
34

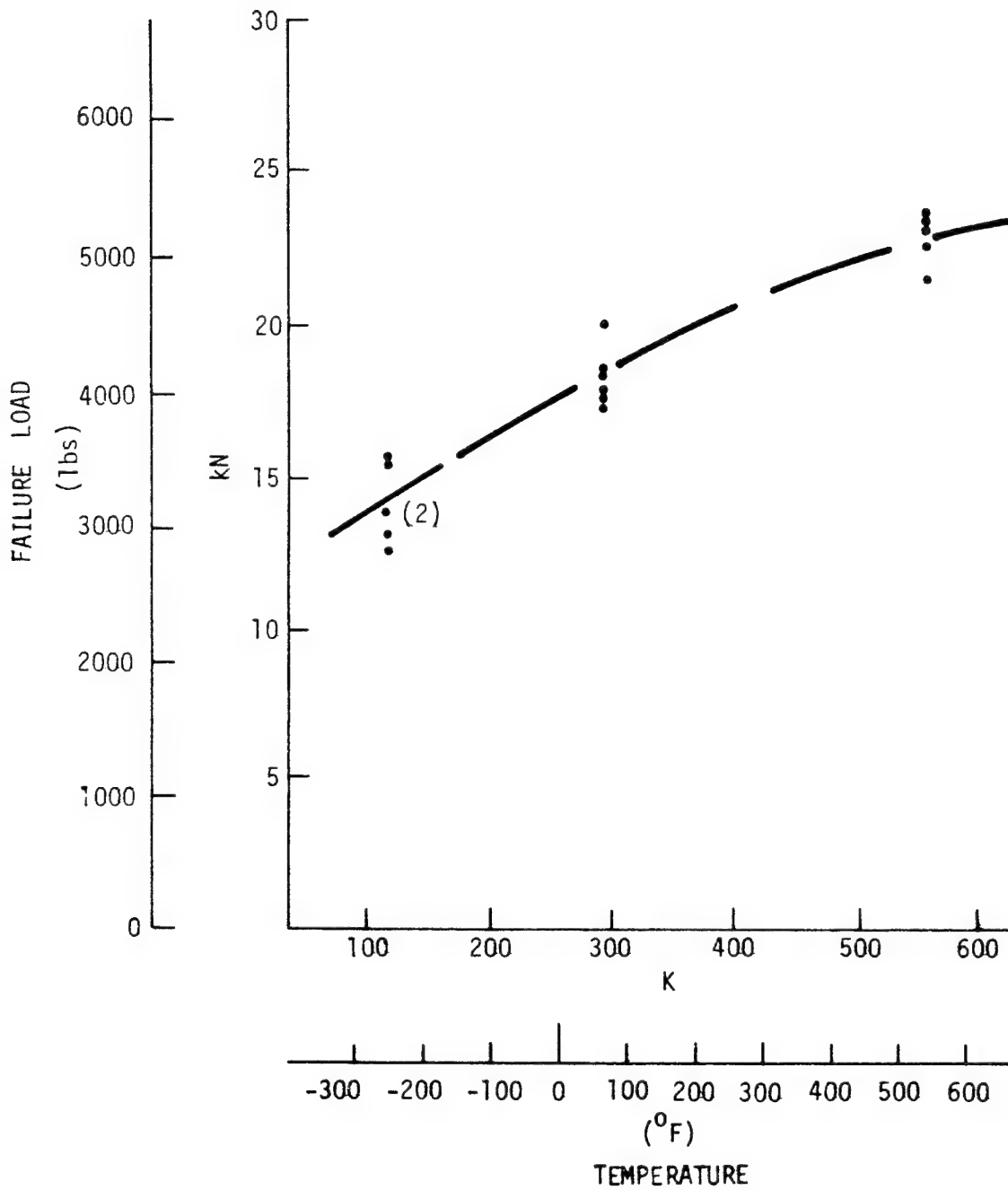Figure 7-7: COMPARISON OF SINGLE- AND DOUBLE-LAP JOINTS GR/PI TO GR/PI JOINTS

35

Figure 7-8: "3 STEP" SYMMETRIC STEP-LAP JOINT, GR/PI TO TITANIUM

JOINT TYPE	PARAMETER	PERCENT CHANGE IN FAILURE LOAD FROM BASELINE					
		SINGLE-LAP JOINTS			DOUBLE-LAP JOINTS		
		116K (-250°F)	294K (70°F)	561K (550°F)	116K (-250°F)	294K (70°F)	561K (550°F)
Gr/PI-Gr/PI	Increased Adherend Stiffness	63	47	150	-1	10	76
	Stacking Sequence (+45/0/90)	—	48	—	-1	0	49
	Stacking Sequence ($0_3/\pm45_3/90_3$)		49		-30	-13	15
	Unbalanced Adherends	-29	-19	6	-9	-12	-15
	Increased Adherend Thickness	—	40	—	—	5	26
	Tapered Adherends ▷1	—	24	—	—	22	7
Gr/PI Ti	Stacking Sequence (±45/0/90)	—	—	—	82	19	4

BASELINE CONFIGURATIONS:

	LAYUP	LAP LENGTH	THICKNESS (Gr/PI-Gr/PI)	THICKNESS (Gr/PI-Ti)
Single Lap	(0/±45/90)	50.8 mm (2.0 in.)	1.52 mm (.06 in.)	———
Double Lap	(0/±45/90)	33.0 mm (1.3 in.)	3.05 mm (.12 in.)	1.52 mm (.06 in.)

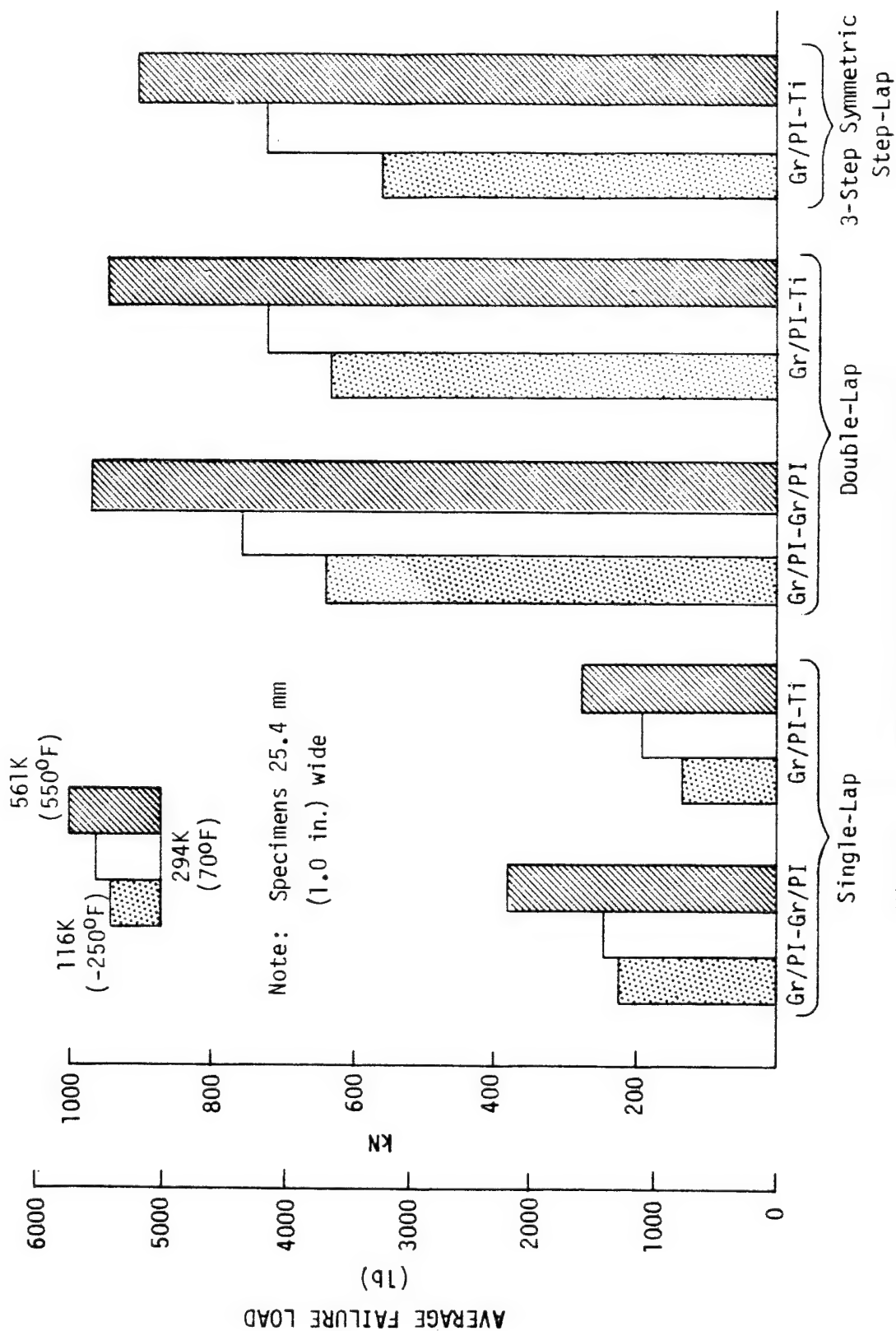▷1 Tapered Adherends Baseline is the Increased Adherend Thickness Configuration

37

Figure 7-9: MAXIMUM JOINT LOADS ACHIEVED

8.0 ADVANCED BONDED JOINTS

Based on the standard bonded single- and double-lap joint testing, several advanced joint design concepts were defined which showed promise of improving the joint efficiency. Concepts selected for testing were preformed adherends, scalloped adherends and two hybrid systems. Standard single- and double-lap bonded joints were made from the same material lot and tested to provide a baseline for comparing the performance of the advanced joint concepts.

The preformed adherend concept consists of a single lap joint with the adherends angled at the lap ends (see Fig. 8-1). Finite element analyses (Ref. 4) have shown that preforming the adherends reduces the stress concentrations in the joint, thus increasing the joint strength. The reduction in peak stresses results from reducing the angle between the line of action of the applied load and the bond line. This in turn reduces the applied bending moments in the adherends and the peak shear and peel stresses in the joint.

Scalloping the ends of the adherends (see Fig. 8-1) was expected to improve the joint strength by reducing the peel stress concentrations at the end of the lap.

The two hybrid systems consisted of: 1) S-glass/PI fabric softening strips and 2) Gr/PI fabric layers placed between the adherends at the joint interface (see Fig. 8-1). These layers were intended to reduce the peak shear and peel stresses in the joint and thus allow a greater load transfer between the adherends.

The advanced bonded joint test matrix is given in Table 8-1. Specimen configurations are as shown in Figure 8-1. All specimens were conditioned by soaking at 589K (600°F) in a one atmosphere environment (air) for 125 hr prior to test. Tests were conducted at 116K, 294K and 561K (-250°F, 70°F and 550°F). A total of 191 specimens were tested.

39

8.1 Advanced Joint Test Results

Results of the preformed adherend tests demonstrate that preforming the adherends of a single-lap joint gives a significant increase in load carrying capability. Figures 8-2 and 8-3 show the effect of preforming for temperatures of 294K (70°F) and 561K (550°F). The average failure load for each lap length is normalized by the average failure load for the baseline (straight adherends) configuration (from the advanced joint test matrix) with the same lap length. In all cases, preforming the adherends increased the average failure load. Increases ranged from 92% to 262% at 294K (70°F) and from 46% to 234% at 561K (550°F). No comparisons were made at 116K (-250°K) because there was no baseline data at this temperature; however, results similar to the 294K (70°F) tests would be expected. As would be expected from these curves the joint efficiencies of the preformed adherend specimens were higher than those of the single-lap standard joints, ranging from 0.27 to 0.68.

In contrast to the standard joints, the preformed adherend specimens had failure loads at elevated temperature which were in all cases lower than those at room temperature. The results for the 116K (-250°F) specimens were not as consistent, in some cases falling above the room temperature loads, sometimes between the room and elevated temperature loads and in some cases below the elevated temperature failure loads. These results may be in part due to the large scatter in the failure load data.

Several failure modes were exhibited by the preformed adherend specimens as outlined in Table 8-2. The failure modes changed from a purely intralaminar peel failure in the ply next to the joint interface, to severe delaminations and peel failures through the adherend thickness, to a failure outside of the joint at the preform bend as the lap lengths and preform angles increased. This change in failure modes may explain why the longer lap length specimens showed smaller improvements in strength over the baseline joints than the shorter lap length specimens (see Figs. 8-2 and 8-3). This result was the reverse of that expected from the results of testing by Sawyer and Cooper (Ref. 4).

40

The effects of scalloped adherends and fabric interfaces are summarized in Table 8-3. Shown are the percent changes in failure load with respect to the appropriate baseline single- and double-lap joints.

Scalloping the single-lap joints gave a slight drop in failure load while scalloping the double-lap joints resulted in an average increase of 17% in failure load. The difference between these two cases can be attributed to the different failure mechanisms of a single versus double-lap joint. The failure in a single-lap joint is governed by both the moment introduced in the joint and by peel stresses. The failure in the double-lap joints is governed primarily by the peel stresses in the inner adherend at the end of the lap. Since scalloping the ends of the adherends was designed to reduce the peel stresses at the end of the lap, it would be expected that the double-lap joints would be more affected by scalloping than single-lap joints.

Failure loads versus lap length for the Gr/PI fabric interface, and S-glass fabric interface specimens tested at room and elevated temperature are compared to baseline data in Figures 8-4 and 8-5. Placing fabric interfaces, S-glass/PI and Gr/PI, between the single-lap joint adherends resulted in 28% to 76% increases in average failure load (see Table 8-2) except for the 25.4 mm (1.0 in.) lap length S-glass/PI specimens, which showed no significant change in strength. The increase in strength can be attributed to a reduction in peak shear and peel stresses due to the "softer" interface materials. Most of the fabric interface specimens delaminated between the two fabric plies, as opposed to delaminating in the adherends as was the case for the standard joints.

The temperature dependence of the joint strengths for the scalloped adherend and fabric interface joints was less than that for the standard joints. In general, there was no significant difference between the failure loads for the room and elevated temperature cases for these joints, with the average difference being a 5% increase from room to elevated temperature. For the few cases where there was a significant difference the elevated temperature loads were greater than the corresponding room temperature failure loads.
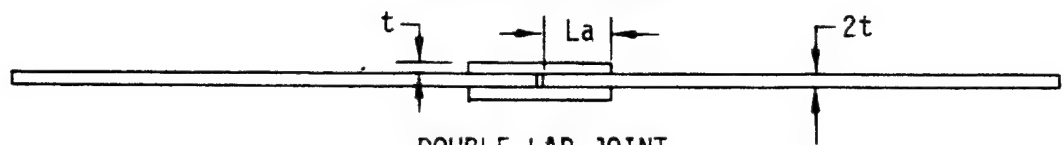
8.2 Advanced Joint Conclusions

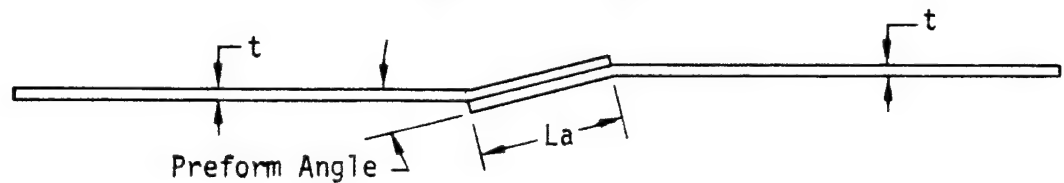The following conclusions have been drawn regarding advanced joint concepts.

o   Single-lap joints with preformed adherends showed a large increase in strength over single-lap joints with straight adherends. The greatest percentage increase in strength was exhibited by the shortest lap length tested.

o   Adding a fabric interface between single-lap joint adherends, either S-glass/PI or Gr/PI, results in a significant increase in joint strength. This is an effective method for improving joint performance.

o   Scalloping the adherends of a single-lap joint does not significantly improve joint strength. Scalloping the ends of the outer adherends of a "Gr/PI-Gr/PI" double-lap joint results in an increase in failure load. This, however, is a costly method for achieving a modest increase in joint performance and does not appear to be practical. Tapering the ends of the adherends is a more cost effective method of achieving the same improvement in double-lap joint strengths.
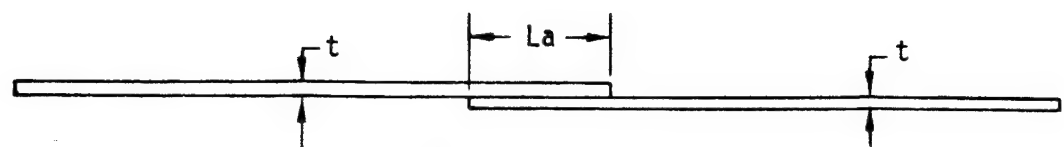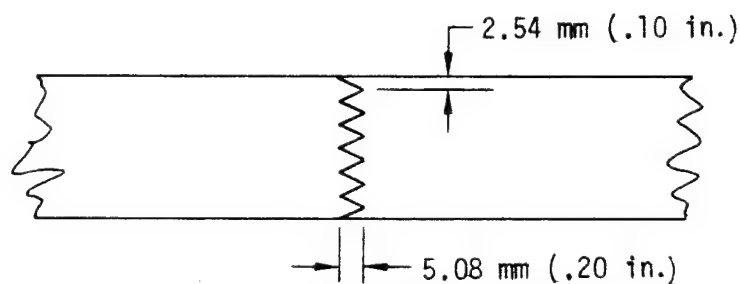
SINGLE-LAP JOINT

DOUBLE-LAP JOINT

PREFORMED SINGLE-LAP JOINT

Preform Angle

2.54 mm (.10 in.)

5.08 mm (.20 in.)

SCALLOPED ADHEREND DETAIL

2 Plies S-Glass/
PI Cloth (+45°)

1.2 mm
(.05 in.)

La + 25.4 mm (1.0 in.)

S-GLASS/PI FABRIC INTERFACE DETAIL

1 Ply Gr/PI Fabric
(0/90) (2 Places)

La
+ 25.4 mm
(1.0 in.)
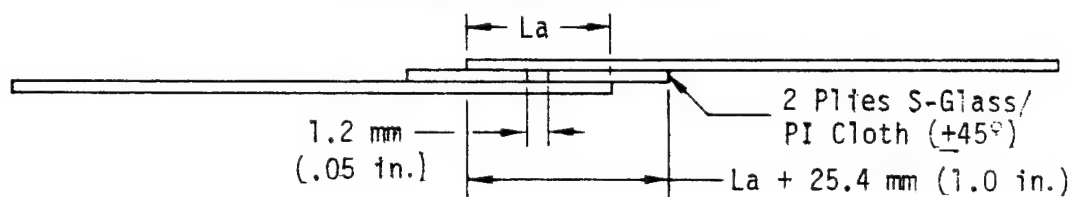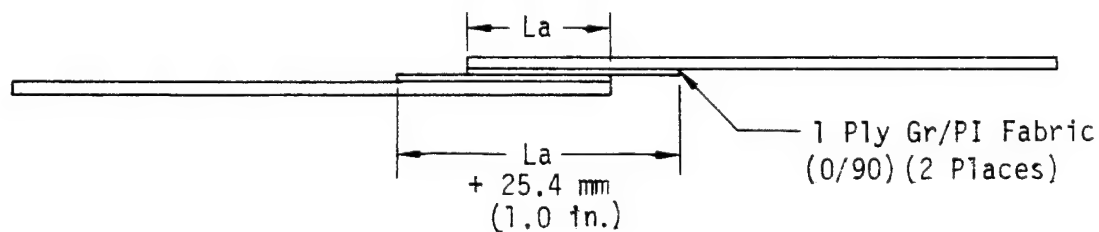
GR/PI FABRIC INTERFACE DETAIL

All Specimen Widths = 25.4 mm (1.0 in.)

Figure 8-1: ADVANCED JOINT CONFIGURATIONS

43

Table 8-1: ADVANCED BONDED JOINT TEST MATRIX

	LAP LENGTH (La) mm (in.)						ADHEREND THICKNESS (t) mm (in.)		TEMPERATURE K (°F)			NO. OF TESTS
	25.4 (1.0)	50.8 (2.0)	76.2 (3.0)	20.3 (0.8)	33.0 (1.3)	45.7 (1.8)	1.02 (.04)	1.52 (.06)	116 (-250)	294 (70)	561 (550)	
PREFORMED ADHERENDS SINGLE-LAP 5°	•	•	•					•	•	•	•	27
10°	•	•	•					•	•	•	•	27
15°	•	•	•					•	•	•	•	27
SCALLOPED ADHERENDS SINGLE-LAP	•	•	•					•		•	•	20
SCALLOPED ADHERENDS DOUBLE-LAP				•	•	•	•			•	•	18
S-GLASS/PI FABRIC INTERFACE SINGLE-LAP	•	•	•					•		•	•	20
GR/PI FABRIC INTERFACE SINGLE-LAP	•	•	•					•		•	•	20
BASELINE SINGLE-LAP	•	•	•					•		•	•	20
BASELINE DOUBLE-LAP				•	•		•			•	•	12

TOTAL 191

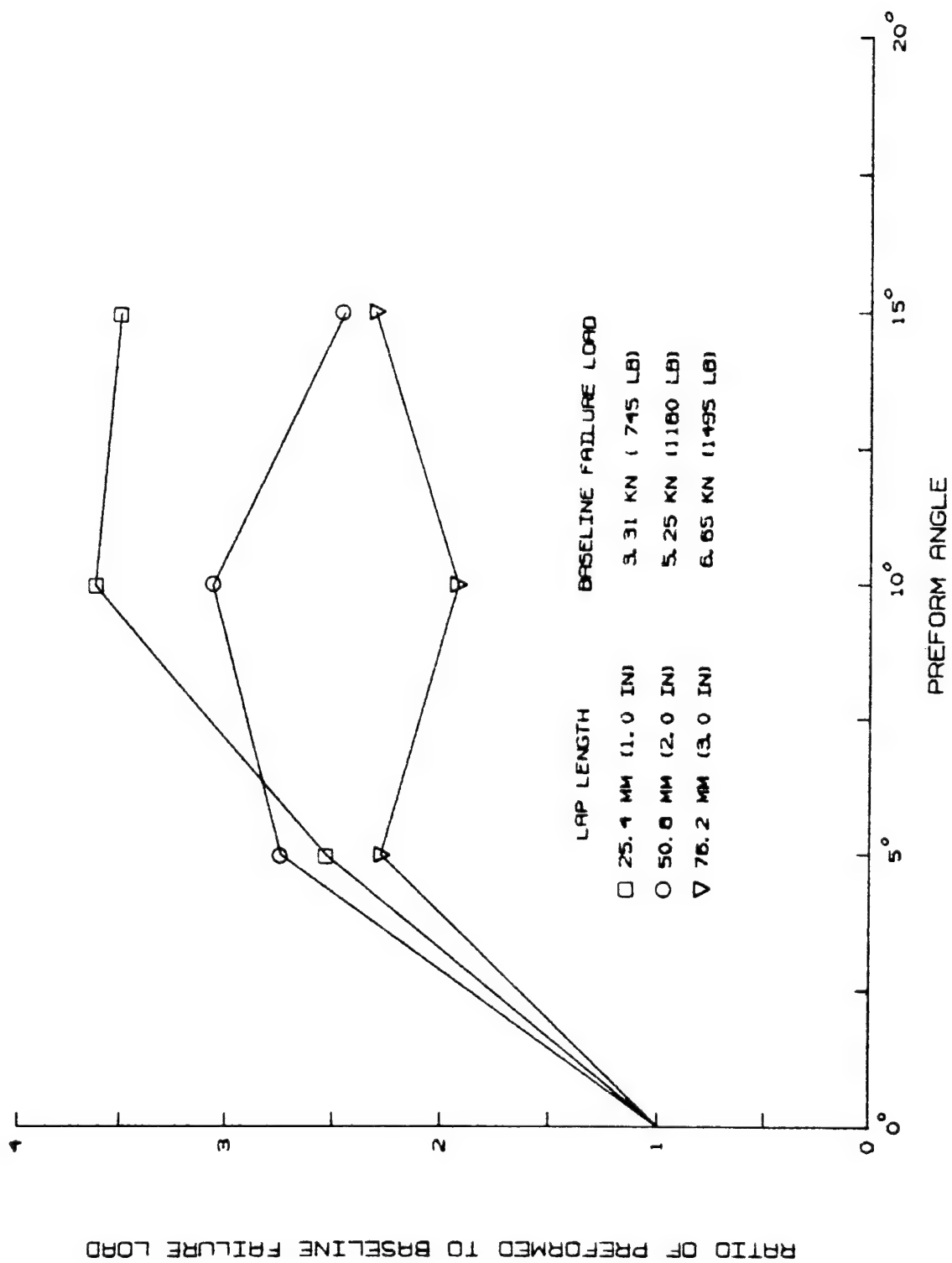NOTE: All Layups $(0/\pm45/90)_{NS}$

44

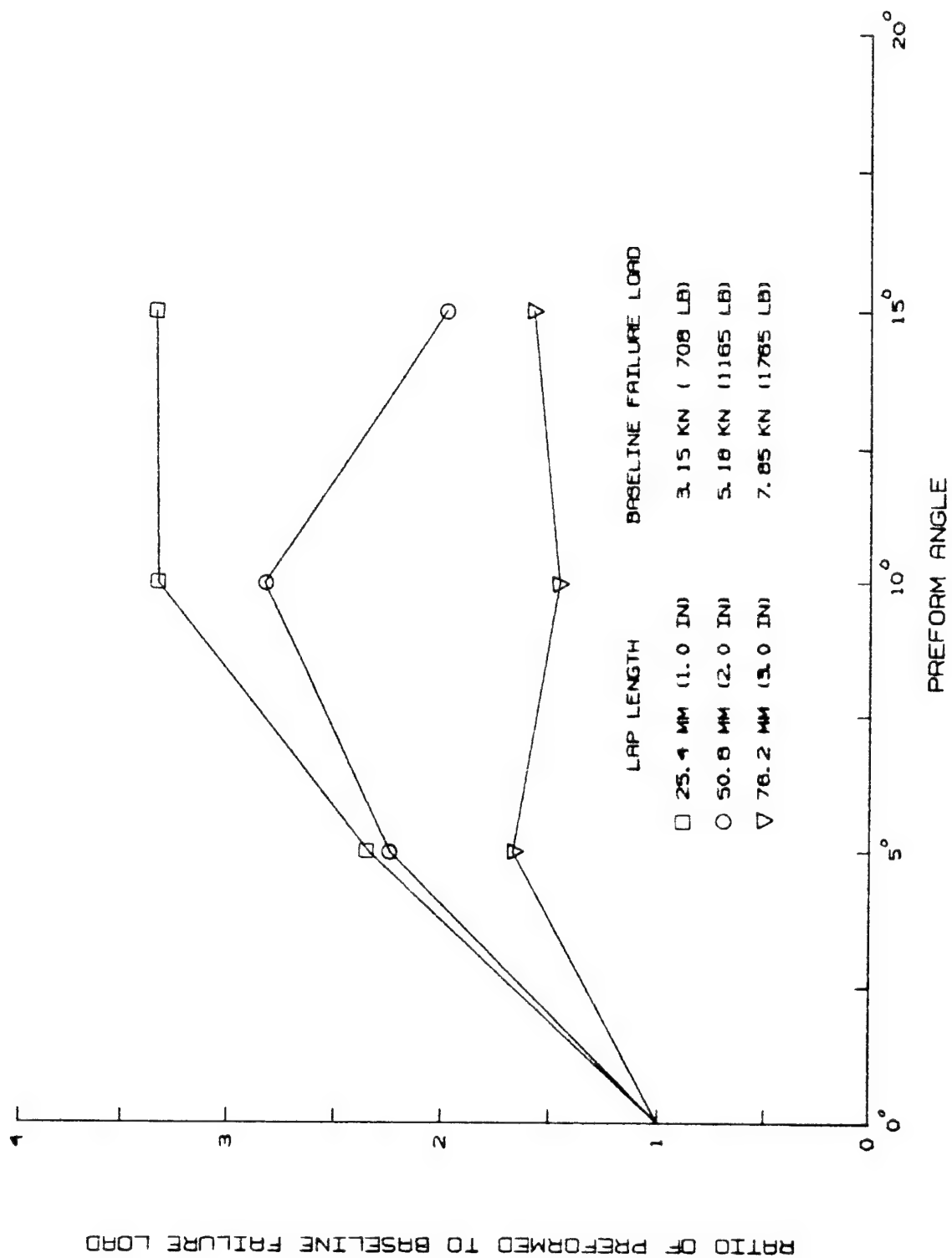Figure 8-2: EFFECT OF PREFORMED ADHERENDS
294K (70°F)

45

Figure 8-3: EFFECT OF PREFORMED ADHERENDS
561K (550°F)

46

Table 8-2: PREFORMED ADHEREND FAILURE MODES

SPECIMEN CONFIGURATION	TEST NO.	LAP LENGTH mm (in.)	FAILURE MODE NUMBERS		
			116K (-250°F)	294K (70°F)	561K (550°F)
5° Preformed	1a	25.4 (1.0)	1	1	1
	1b	50.8 (2.0)	1	1	1
	1c	76.2 (3.0)	2	1	1
10° Preformed	2a	25.4 (1.0)	1	1	1
	2b	50.8 (2.0)	3	2	2
	2c	76.2 (3.0)	3	2, 3	3
15° Preformed	3a	25.4 (1.0)	1, 2	1	1
	3b	50.8 (2.0)	3, 4	3	3
	3c	76.2 (3.0)	4	4	1, 4

Failure
Mode No.   Failure Mode

1.   Intralamina failure in adherend first ply +
      adherend-adhesive interface failure

2.   Interlamina failure in adherend + some tensile
      failures of individual plies

3.   Interlamina failure through adherend + tensile
      failures of individual plies

4.   Tensile failure of adherend at preformed bend

Table 8-3: EFFECT OF ADVANCED JOINT CONCEPTS

| PARAMETER	LAP LENGTH		PERCENT CHANGE IN FAILURE LOAD FROM BASELINE ADVANCED JOINTS	
	mm	(in.)	294K (70°F)	561K (550°F)
Single-Lap Scalloped Adherends	25.4 50.8 76.2	(1.0) (2.0) (3.0)	-21 1 -7	-8 8 4
Double-Lap Scalloped Adherends	20.3 33.0 45.7	(0.8) (1.3) (1.8)	21 11 ▷1	17 17 ▷1
Single-Lap S-Glass/PI Fabric Interface	25.4 50.8 76.2	(1.0) (2.0) (3.0)	11 76 59	-8 58 28
Single-Lap Gr/PI Fabric Interface	25.4 50.8 76.2	(1.0) (2.0) (3.0)	61 75 65	72 66 40

▷1 No Advanced Joint Baseline Double Lap

48
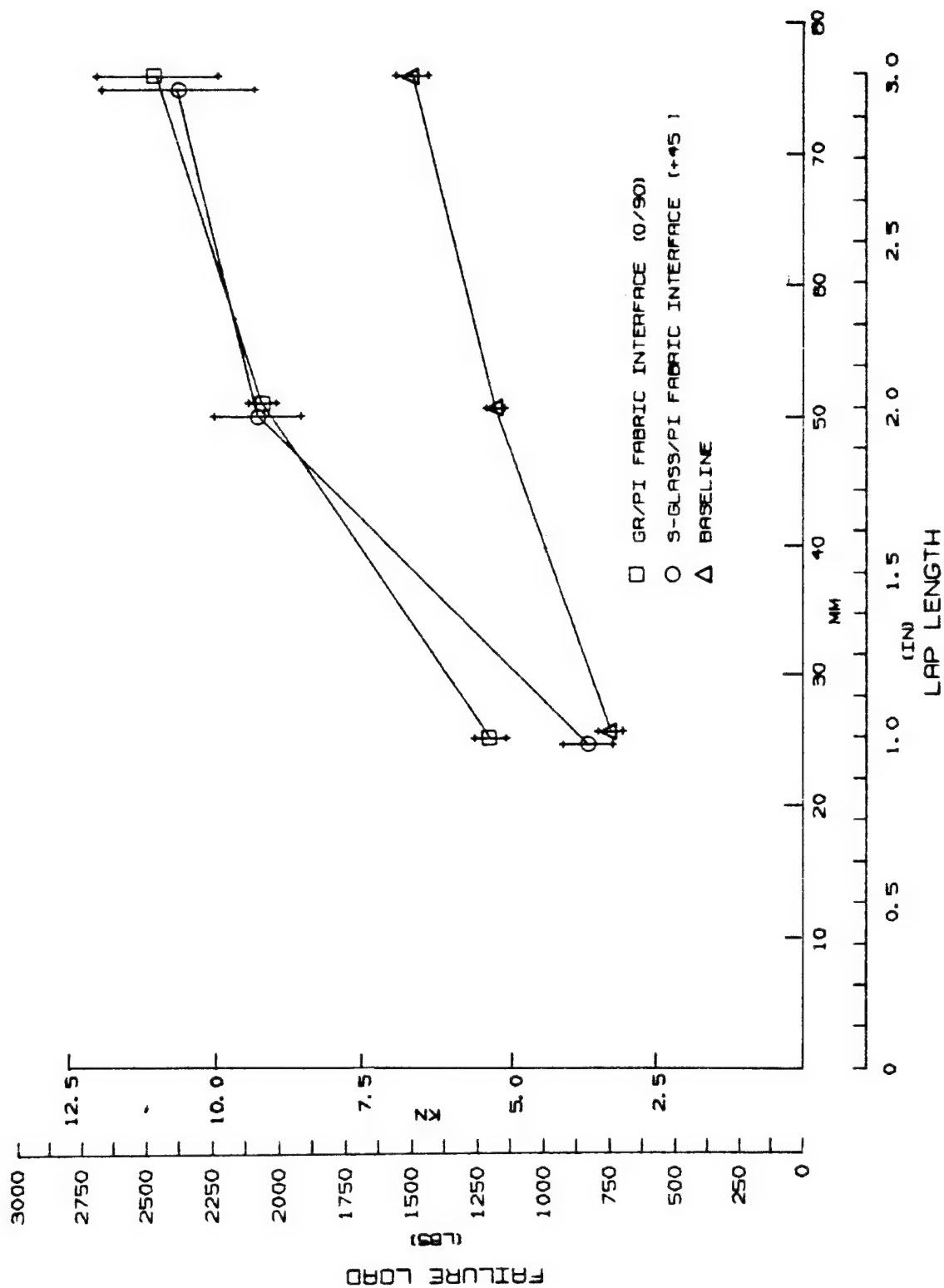
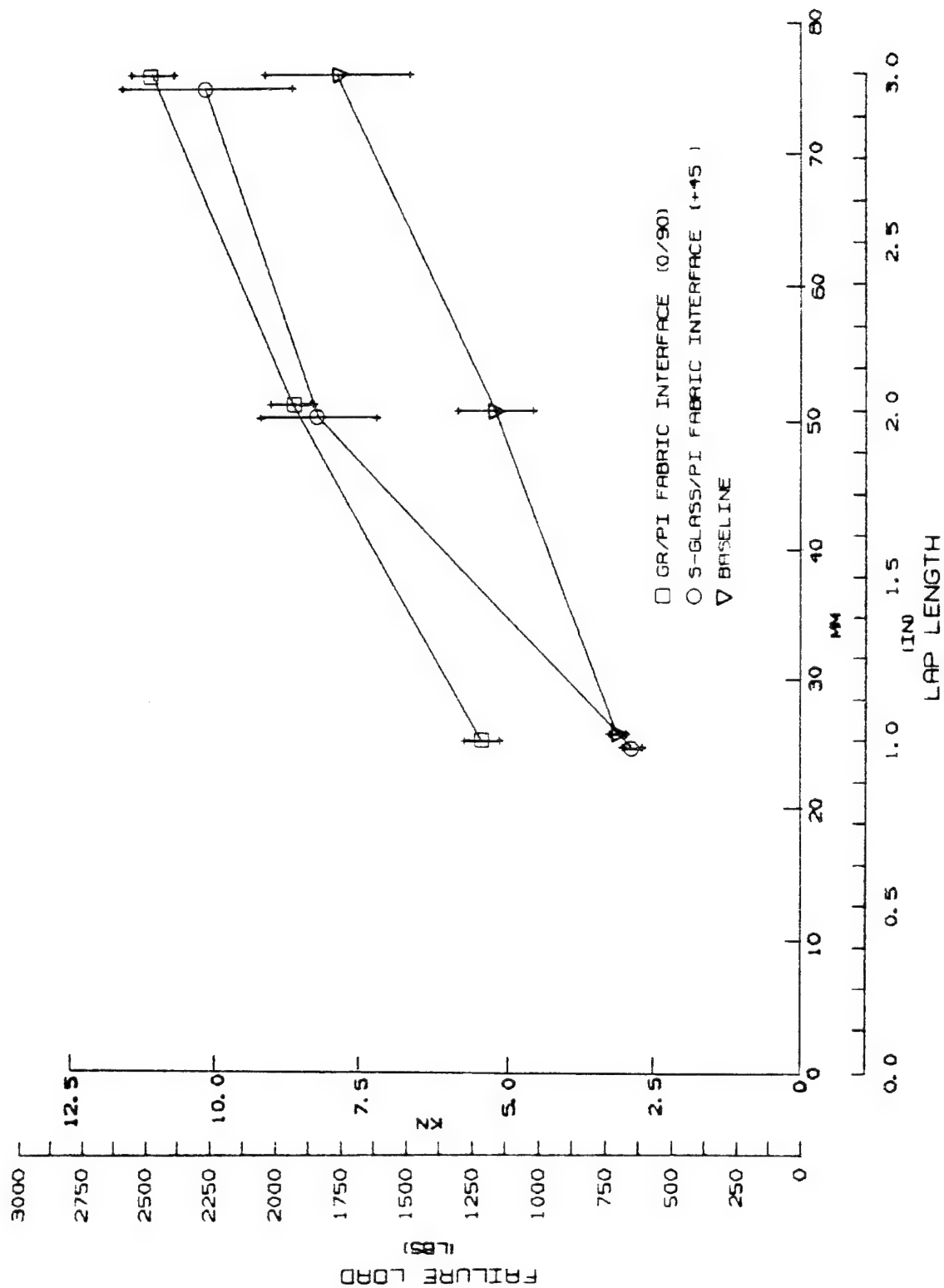Figure 8-4: EFFECT OF FABRIC INTERFACES - SINGLE-LAP JOINTS
294K (70°F)

49

Figure 8-5: EFFECT OF FABRIC INTERFACES - SINGLE-LAP JOINTS
561K (550°F)

50

9.0 TEST/ANALYSIS CORRELATION

9.1 Finite Element Analysis (Boeing IR&D)

Finite element analyses of single- and double-lap joints were performed using Boeing's BOPACE program. Modeling studies were conducted to optimize element size and arrangement and still provide the degree of accuracy needed to predict joint performance trends. Analyses were then conducted of specific joint designs to predict performance trends for various changes in the lamina stacking sequence.

Study of Finite Element Modeling Techniques — Double-Lap Joints

Results of finite element analyses are strongly dependent on element size and modeling techniques. Ideally, smaller elements are required in areas of high stress concentrations; however, smaller elements also result in larger computer usage times and a corresponding increase in cost. Studies were performed to address the following areas and to assess their impact on analysis results.

o   Required element size near stress risers.
o   Acceptability of rezoning to larger elements, away from stress risers.
o   Effect of lamina property averaging when element size exceeds lamina thickness.
o   Possible discretization requirements dictated by lamina and adhesive material interfaces.
o   Number of elements required through the adhesive thickness.
o   Effects of varying longitudinal grid size with the transverse grid fixed and of varying the transverse grid size with the longitudinal grid fixed.
o   Effects of adding adhesive fillets.

The modeling studies were performed using an elastic, geometrically linear analysis of a composite double-lap bonded joint. Results of these analyses suggested the conclusions listed below which were incorporated into subsequent standard joint analyses.

o   The peak shear, axial and peel stresses are not strongly dependent on mesh fineness, although for the coarsest model used some loss of accuracy is necessarily present. This assumes that the stresses are evaluated at some fixed point away from the end of the adherend.

o   Lamina property averaging across large elements essentially results in predicted stresses which are an average of the values for the individual lamina. However deformed structure plots show that a deformation anomaly occurs at junctions between large and small elements where property averaging has been done. This results from the load path eccentricity relative to the larger element size.

o   The magnitude of the gap between the inner adherends has an important influence on stress levels.

o   Near stress concentrations, the value of the stress at the center of the element (or at other internal locations) may differ significantly from those at the edges of elements.

o   A highly refined mesh in the adhesive region is not required. Two elements through the adhesive thickness are sufficient.

o   When comparing results from two models it is important to keep the longitudinal grid size constant.

o   Adding an adhesive fillet would appear to have little effect on joint strength, as the fillet changes the location of the peak peel stress in the inner adherend but does not reduce it.

Standard Bonded Double-Lap Joints

Finite element analyses were conducted on 3 double-lap bonded joint configurations to evaluate various lamina stacking sequences. Model configurations analyzed are shown in Figure 9-1. The first had a very stiff zone, three 0^0

52

lamina adjacent to the adhesive, the second, one 0° lamina adjacent to the adhesive and the third a very soft zone, $\pm45^O$ lamina nearest the adhesive. These analyses were used to predict trends and to compare stress levels in one joint with another. No predictions of failure load or joint strength were made at the time the analyses were conducted.

A comparison of the three joints shows that all have the same extensional stiffness, but the flexural stiffness is quite different. The flexural stiffness is a far less important parameter for double-lap joints than for single lap joints. Each of the joints studied was designed to fail in the joint rather than in the adherend outside the joint. Thus, the adherend laminate is lightly loaded and the critical stresses are the adhesive shear stress, τ_{xz}, and the inner adherend peel stress, σ_z, in the lamina adjacent to the adhesive near the edge of the lap. The latter becomes increasingly important as the adherend becomes thicker.

A comparison of peak shear stresses, τ_{xz}, for the three models is shown in Figure 9-2. There is a reduction in the peak shear stress as the interface layer is made softer in extensional stiffness. A soft buffer next to the adhesive, i.e., the $\pm45^O$ lamina, transfers load more slowly with lower shear stress in the adhesive. This is accomplished by allowing additional shear strain across this soft zone, weakening the condition of equal strain, ε_x, in the adherends and in the splice plates.

A comparison of peak peel stresses, σ_z, for the three models is shown in Figure 9-3. This shows the opposite trend. The peel stresses increase as the interface layer becomes softer, but the increase in a smaller percentage than the reduction in shear stresses.

In conclusion, these analyses indicate that it would be advantageous to have a soft zone (i.e., $\pm45^O$) adjacent to the adhesive. This would produce a decrease in adhesive shear stress, leading to an increase in joint strength provided the peel strength of the laminate is not exceeded.

53

Standard Bonded Single Lap Joints

L. J. Hart-Smith suggests three distinct failure modes in a single lap bonded composite joint: (1) failure of the adherend outside the bonded region because of additional bending stresses, (2) failure of the adhesive in shear, and (3) failure of the composite at the interface near the end of the joint because of "peel" stresses in the adhesive or lamina (Ref. 5).

Examination of the failed single-lap joints tested during this program shows the third type of failure governed in nearly all cases. Therefore, any change that can reduce the peel stress, σ_z, in the adhesive and in the lamina adjacent to the adhesive should increase the efficiency of the single-lap joint.

An elastic, geometrically nonlinear finite element analysis was performed on a "Gr/PI-Gr/PI" single-lap bonded joint. A geometrically nonlinear model was used to account for the large rotations of the joint elements under load. Joint model, boundary conditions and material properties used are shown in Figure 9-4.

The finite element analyses considered two layups for comparison: the first had $(0_3/\pm45_3/90_3)_S$ adherends and the second had $(\pm45_3/0_3/90_3)_S$ adherends. The extensional stiffness of the two layups is the same, but the flexural stiffness of the first is 66% greater than the second. The peak peel stresses are 30% greater for the $(\pm45_3/0_3/90_3)$ layup. Shear stresses in the adhesive did not change significantly between models. Analysis results indicate that if peel stresses are governing the joint failure, increasing the adherend flexural stiffness should increase the joint strength.

9.2 Test/Analysis Correlation

Several analysis methods were evaluated to predict the strengths of the standard bonded joints. Most of the bonded joints failed in an intralaminar peel and/or shear mode. Therefore, most of the analyses in the literature, which

deal primarily with adhesive stress distributions and strengths, were not applicable.

The A4EA single-lap joint analysis code developed by L.J. Hart-Smith (Ref. 5) calculates joint strengths based on adherend bending and peel stresses and on adhesive shear stresses. Test results had shown that the peel strength was the controlling parameter for the single lap joints tested. Therefore the A4EA code was chosen for correlation analysis. Initially the code did not give a good correlation with the test results. The equations used to calculate the moment in the adherends were changed to try to improve the correlations. Two alternate moment equations were substituted into the code. They are the unsimplified moment equation derived by Hart-Smith (Eq. (38) in Ref. 5) and the moment equation derived by Goland and Reissner (Ref. 6). Both equations resulted in significantly improved correlation with the test data. Figure 9-5 shows joint strength predictions based on peel failures for the three moment equations along with the appropriate test data for the 294K (70°F) test temperature. Results for the elevated temperature case were similar. The peel strength predictions depend on the ratio $\sigma_{c_{max}}^2/E_c'$. Since the parameters $\sigma_{c_{max}}$ (adherend or adhesive peel strength) and E_c' (effective adhesive transverse tensile modulus) were not known with any degree of certainty, the above ratio of the parameters was varied to give the best correlation. The value used for this ratio are given on the figure. Correlation was very good at small lap lengths and diverged at the longer lap lengths; however, the performance trend was correct.

An empirical method for the single-lap joints was also developed. It was postulated that failure occurs when the maximum principal stress at the critical point in the adherend reaches a certain value. The critical point is the point in the adherend directly below the end of the joint overlap. The maximum principal stress at this point was calculated based on the actual test results for one lap length. This value of allowable stress was used to predict the failure load for the other lap lengths. Figure 9-7 shows the empirical joint strength predictions for all three test temperatures along with the appropriate test data.

Empirical and A4EA predictions were made for the various single-lap joint configurations tested. The average prediction error for the full Hart-Smith A4EA version was 23% ±18% (avg. ±1 std. dev.), for the Goland and Reissner A4EA version 18% ±13%, and for the empirical technique 24% ±15%.

An empirical method similar to the approach used for the single-lap joints was investigated to predict the strength of double-lap joints. The maximum principal stress was again used as the failure criteria. Figure 9-8 shows the empirical double-lap joint strength predictions for all three test temperatures along with the appropriate test data. The average prediction error for all double-lap joint configurations tested was 24% ±25%.

Joint strength predictions for the "3-step" symmetric step-lap joints were calculated using the A4EGX computer code developed by Hart-Smith (Ref. 7). Due to code problems a prediction was only obtained for the 561K (550°F) case. The predicted failure load was 898 kN/m (5126 lb/in) compared to an average failure load of 901 kN/m (5147 lb/in). Although the predicted load was accurate, the code predicted an adhesive failure, whereas the actual joints appeared to have interlaminar composite failures.
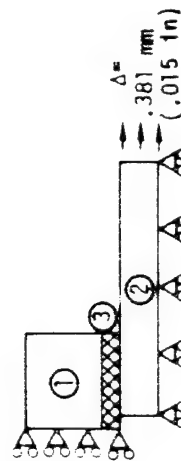
9.3 Test Analysis/Correlation Conclusions

It is concluded that the above bonded joint prediction methods should be viewed only as "rough" prediction techniques. The failure of composite bonded joints is characterized by several failure modes: adherend tensile and intra-lamina shear/peel, and cohesive failure of the adhesive. Due to the complexity of the failure modes, and the highly nonuniform stress distribution, predictions of joint strength become extremely difficult. Also, the material properties required for a joint strength analysis, adherend and adhesive peel strengths, transverse tensile moduli, etc., are difficult to measure accurately.

Although numerous researchers have investigated the state of stress within a bonded composite joint, few have made an attempt to predict actual failure

loads. Also, most of these prediction techniques assume a failure of the adhesive, and do not address the problem of interlamina composite adherend failures.

The A4EA single-lap joint analysis code had good correlation with the test data when appropriate modifications are made. However, work needs to be done to extend this analysis code to joint configurations such as tapered adherends, dissimilar adherend materials, altered laminate stacking sequences and fabric interfaces.

The empirical techniques, while giving reasonable correlations, require that at least one set of tests be performed before predictions can be made. Further work needs to be done to improve this technique for parameter changes other than lap length and thickness.

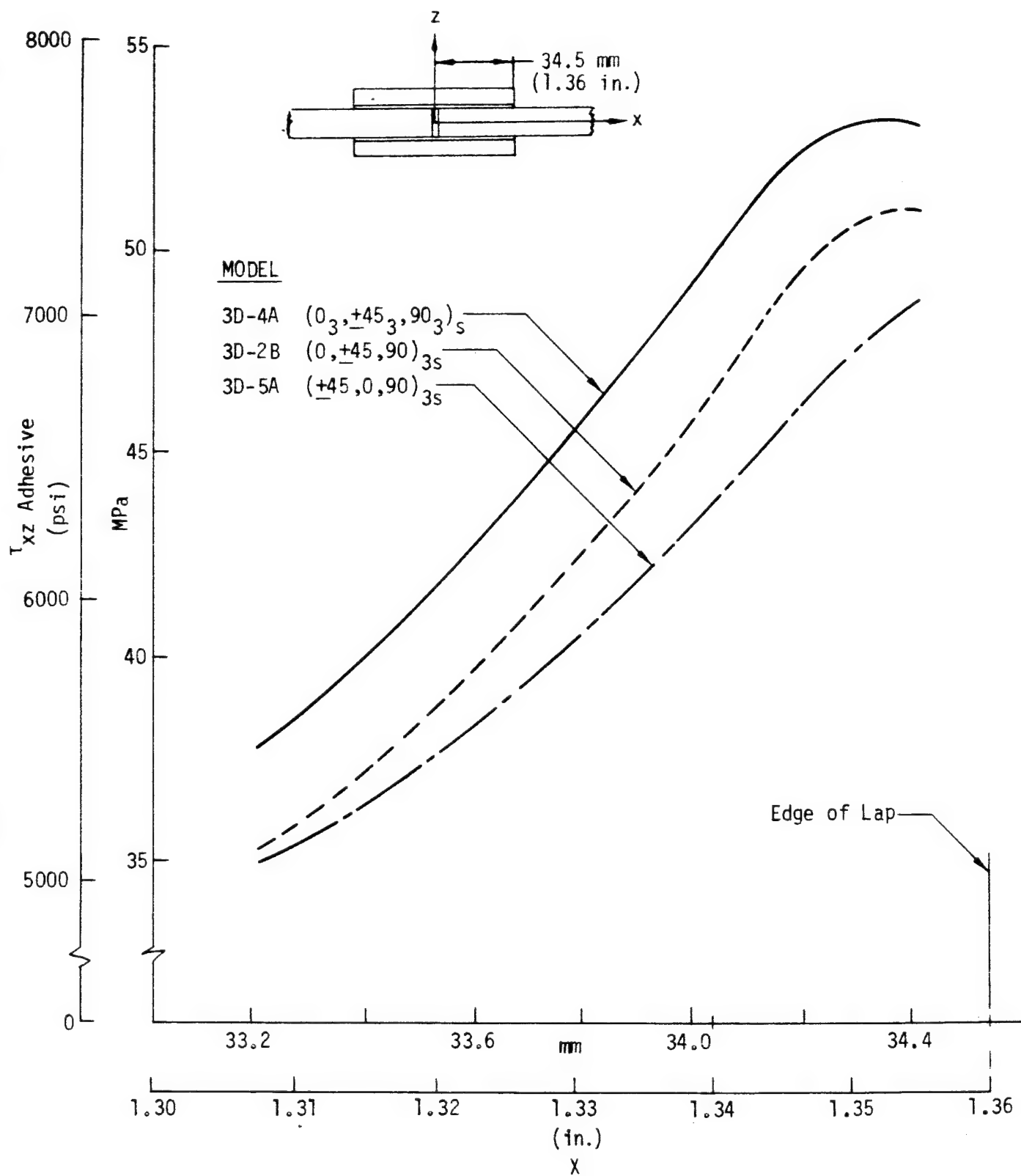Figure 9-1: DOUBLE-LAP BONDED JOINT CONFIGURATION

58

Figure 9-2:   SHEAR STRESS IN ADHESIVE - τ_{xz} vs x

59
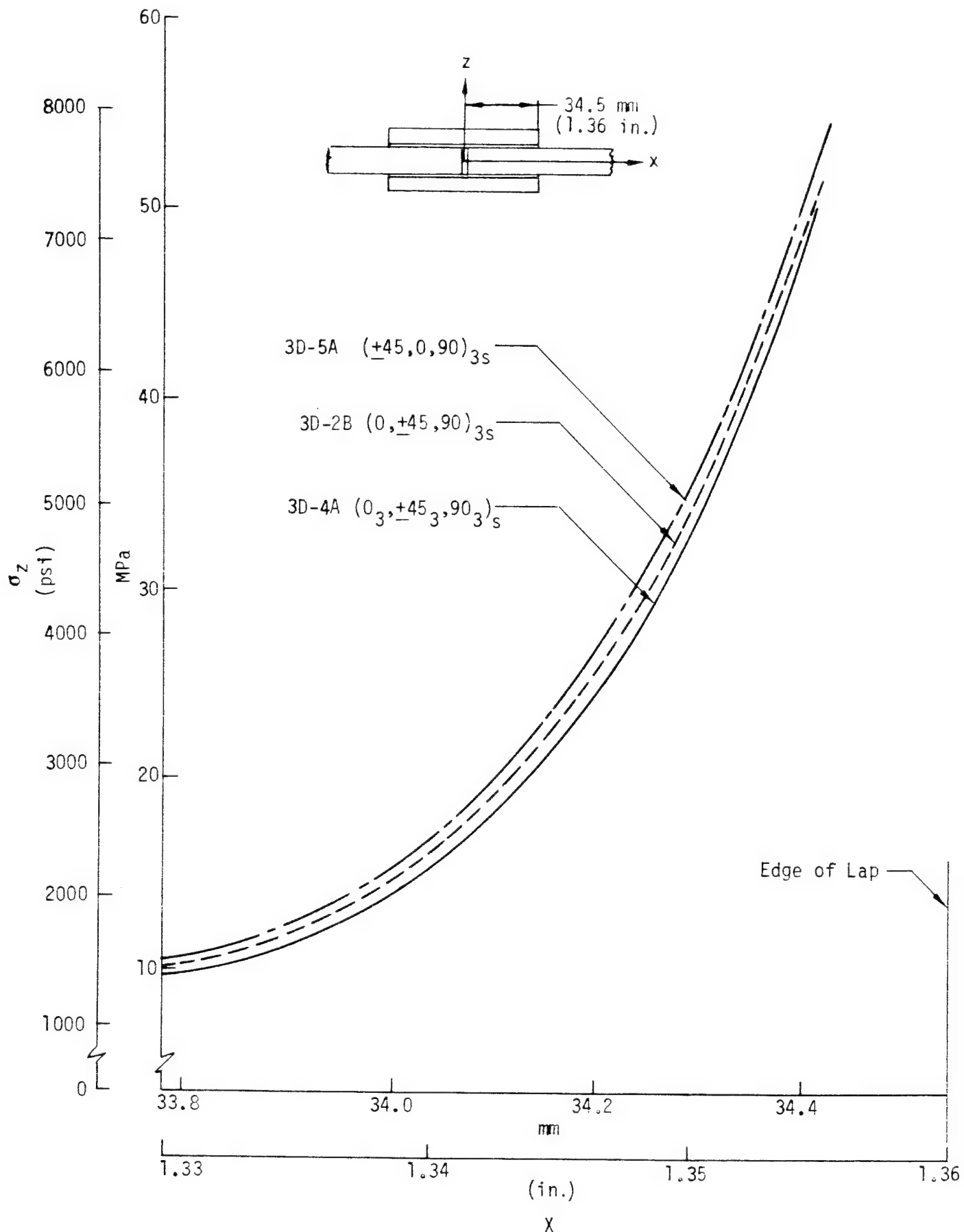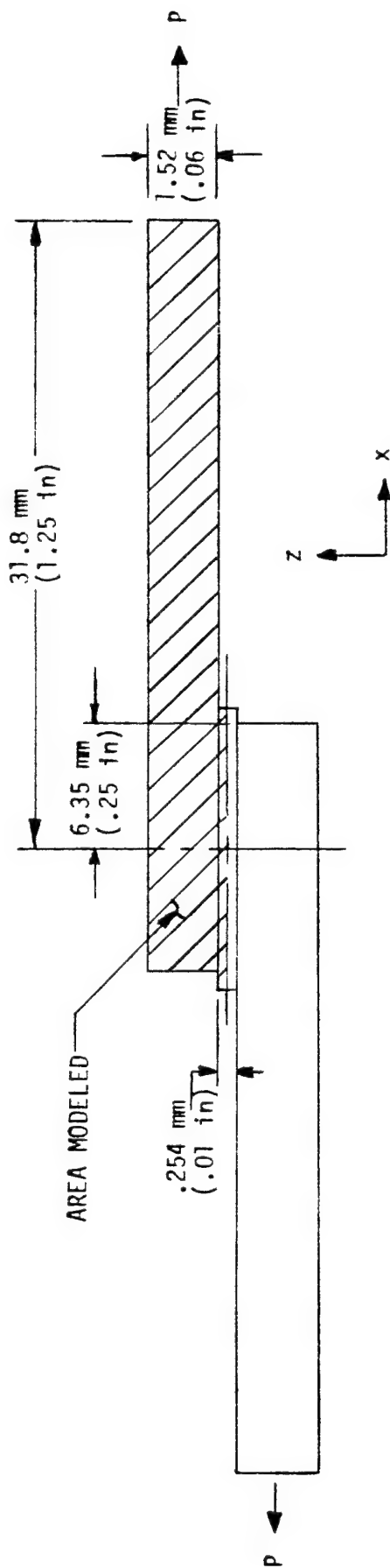
Figure 9-3:   PEEL STRESS IN LAMINA NEAREST ADHESIVE - σ_z vs x

MATERIAL DATA

① GR/PI

$E_1 = 137$ GPa (20×10^6 psi)
$E_2 = 11$ GPa (1.6×10^6 psi)
$u = .25$
$G_{12} = 5.8$ GPa ($.85 \times 10^6$ psi)

② ADHESIVE $G = 2.1$ GPa ($.309 \times 10^6$ psi)
(Assumed Homogeneous & Isotropic)

BOUNDARY CONDITIONS

A & C $\vec{u}_A = -\vec{u}_C$
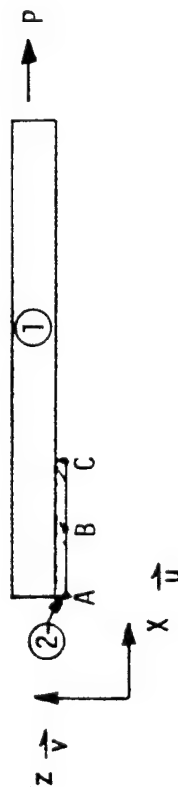
B $\vec{u} = \vec{v} = 0$

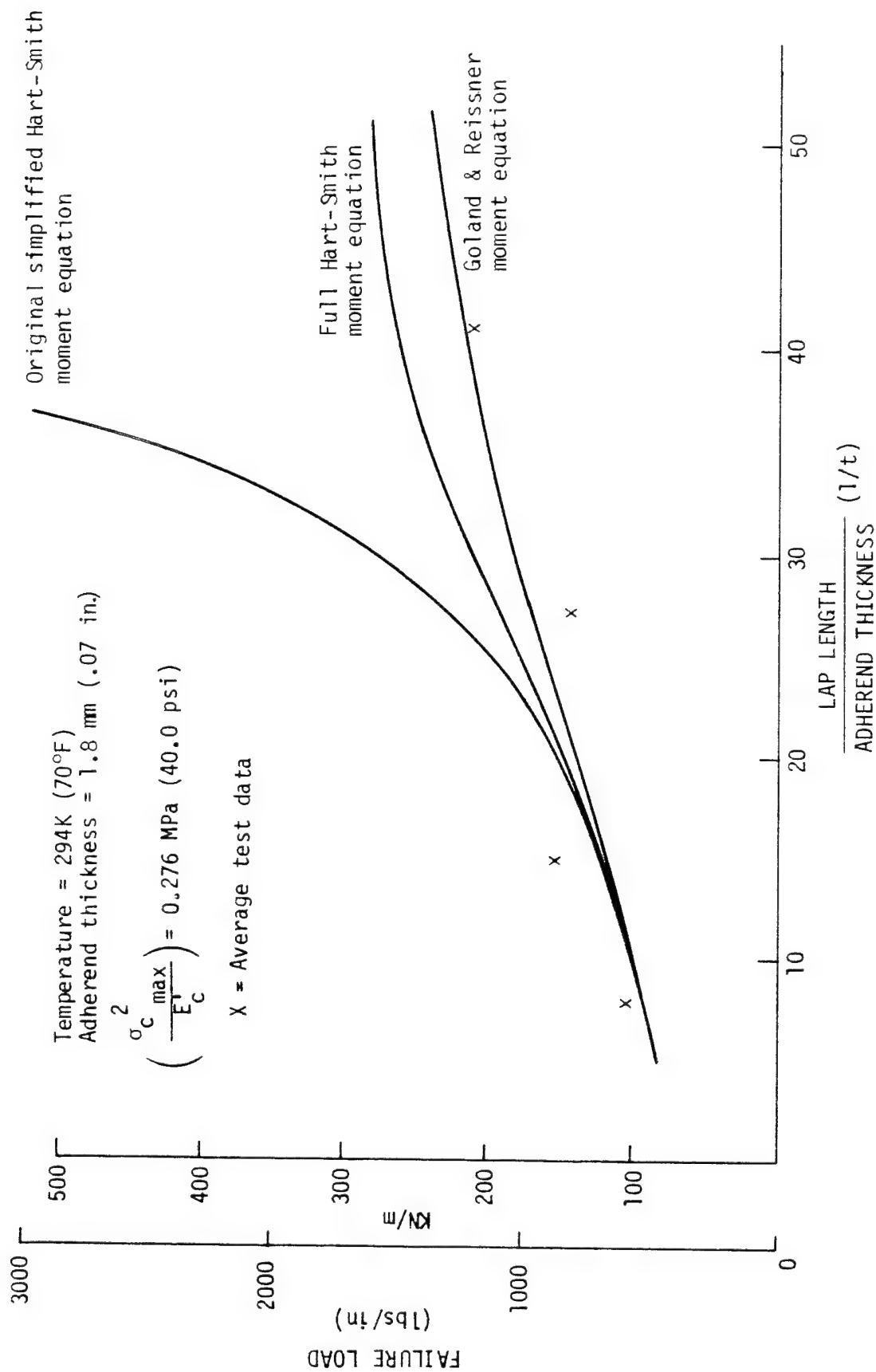Figure 9-4: GR/PI BONDED SINGLE-LAP JOINT

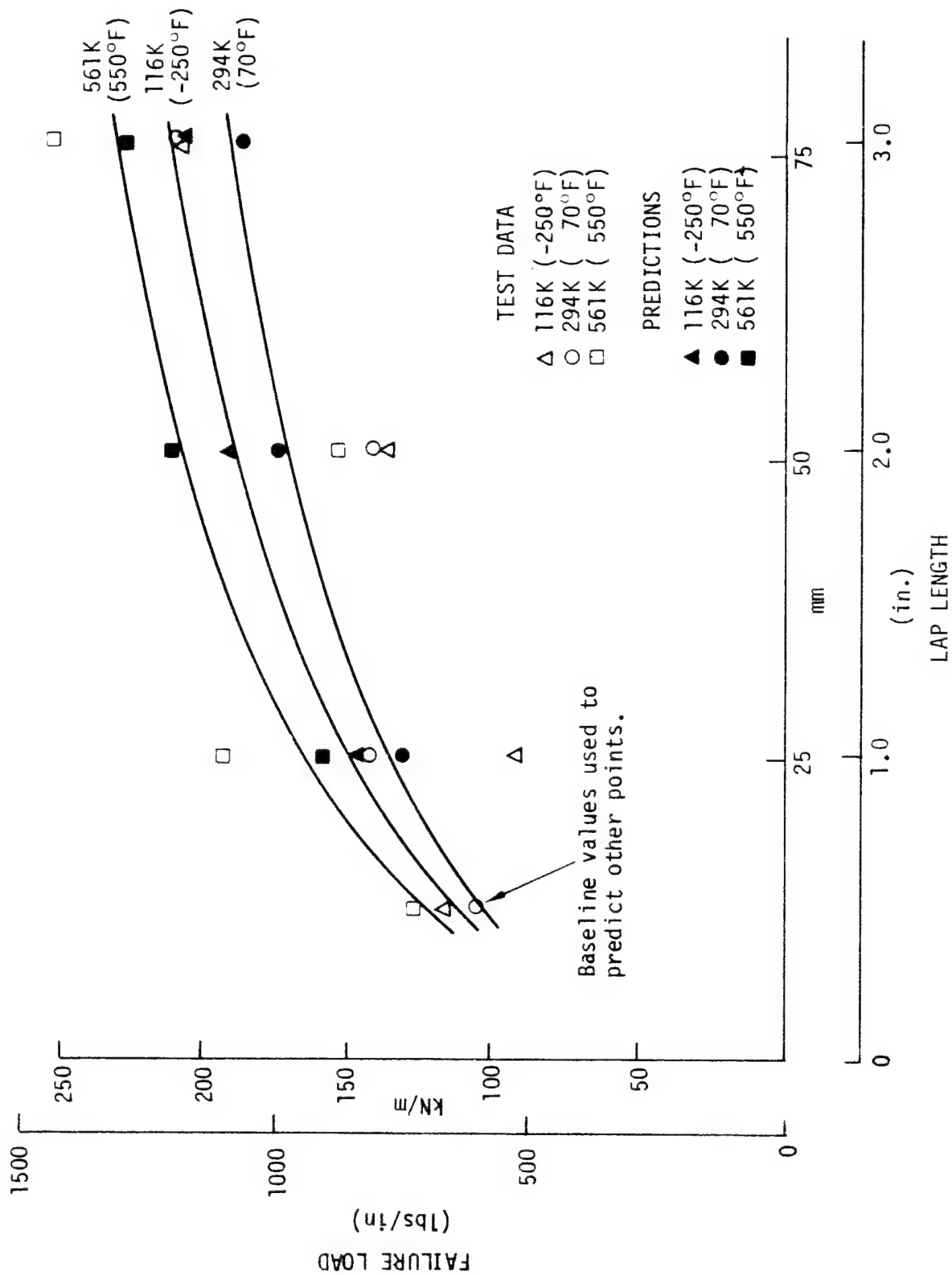Figure 9-5: PREDICTED STRENGTH OF SINGLE-LAP JOINTS - PEEL FAILURES

62

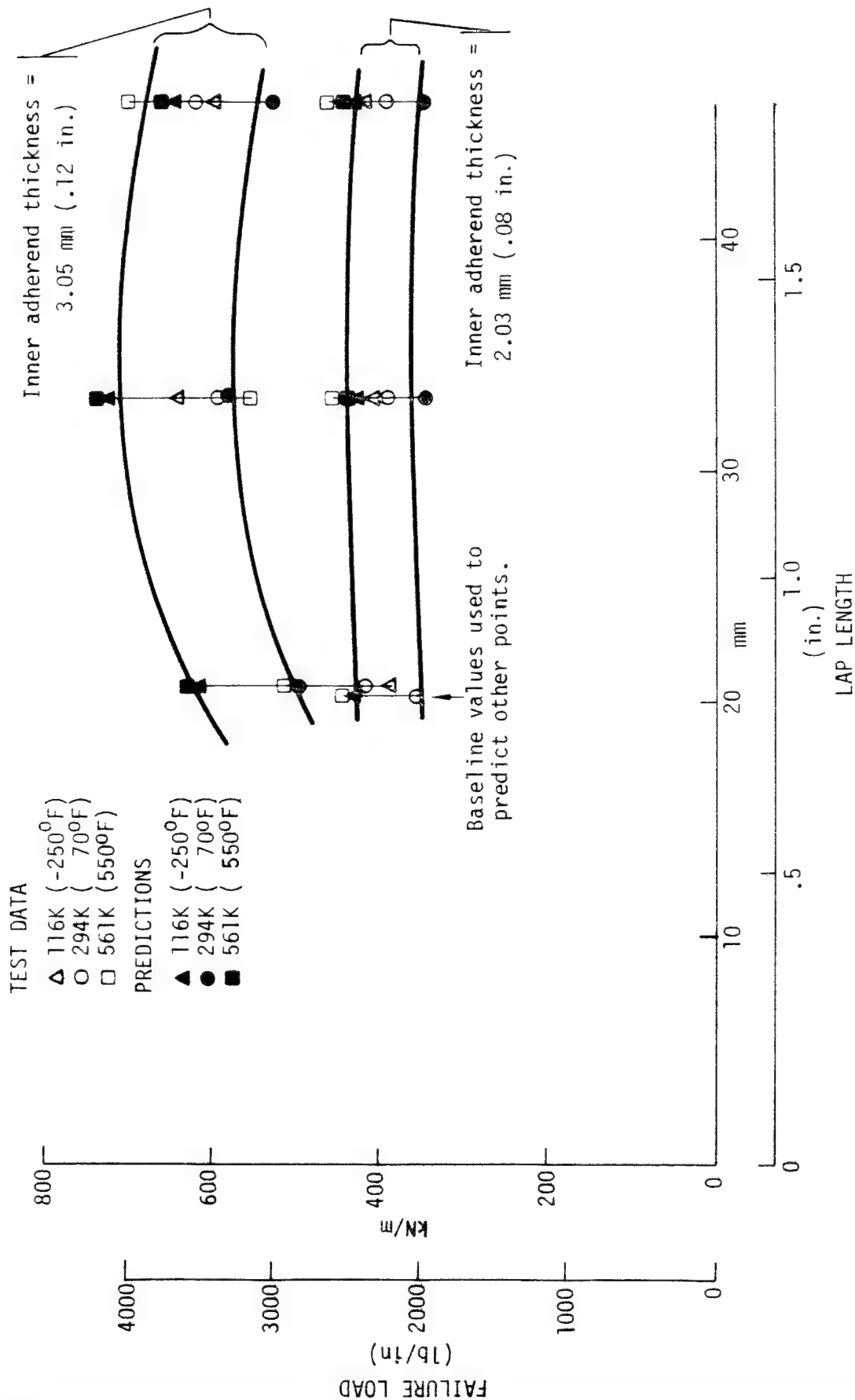Figure 9-6: EMPIRICAL CORRELATION - SINGLE-LAP JOINTS

63

Figure 9-7: EMPIRICAL CORRELATION - DOUBLE-LAP JOINT

64

10.0   CONCLUSIONS/RECOMMENDATIONS

The following conclusions have resulted from this program:

o   Bonded "Gr/PI-Gr/PI" and "Gr/PI-titanium" joints can be designed and fabricated to carry loads of the magnitude expected for advanced aerospace vehicles over the 116K (-250°F) to 561K (550°F) temperature range.

o   Joint strength for these material combinations increases with:

- increased lap length
- increased temperature
- increased adherend stiffness
- increased adherend thickness
- adherend tapering
- ±45° plies at the joint surface

o   Hybrid systems (fabric interfaces) provide a simple and effective way to increase joint strength.

o   Preformed adherends significantly increase single-lap joint strength. Large deflections under load cause joints with preformed adherends to act as scarf joints.

o   A7F has a shear strength greater than 8.3 MPa (1200 psi) in the 116K (-250°F) to 589K (550°F) temperature range.

o   Finite element analyses of composite bonded joints can successfully predict joint performance trends.

o   Composite bonded joint strength prediction techniques are at this time limited to simple joint configurations and result in "rough" predictions only.

Based on the results and conclusions derived from this program, the following areas for further work on bonded composite joints are recommended:

o   The combined effect of the following joint parameters and configurations investigated in this program should be explored in order to further increase joint strengths:

   - hybrid systems (fabric interfaces)
   - adherend tapering
   - increased stiffness
   - ±45° plies at joint interfaces

o   Hybrid systems for double-lap joints should be investigated.

o   Further work in predicting bonded joint strengths needs to be undertaken in order to improve confidence in using bonded composite joints for designs.   The complex failure modes of composite adherends are not well understood.   Since the interlamina strengths of composite laminates are low, composite bonded joints are susceptible to peel and/or interlamina shear failures, as opposed to an adhesive failure.

o   Preformed joints should be considered for use in two areas: 1) an internal structural attachment or in external joints which can be covered by fairings and 2) as a possible replacement for the ASTM D-1002 lap shear specimens so that the results approach the true adhesive shear strength (because of the reduced peel stresses).

1. Report No. NASA CR-3602	2. Government Accession No.	3. Recipient's Catalog No.
4. Title and Subtitle Test and Analysis of Celion 3000/PMR-15, Graphite/ Polyimide Bonded Composite Joints - Summary		5. Report Date January 1983
		6. Performing Organization Code
7. Author(s) J. B. Cushman, S. F. McCleskey, S. H. Ward		8. Performing Organization Report No.
		10. Work Unit No.
9. Performing Organization Name and Address BOEING AEROSPACE COMPANY Engineering Technology Post Office Box 3999 Seattle, Washington 98124		
		11. Contract or Grant No. NAS1-15644
		13. Type of Report and Period Covered Contractor Report
12. Sponsoring Agency Name and Address National Aeronautics and Space Administration Washington, D.C. 20546		
		14. Sponsoring Agency Code

15. Supplementary Notes

Technical Representative: Paul A. Cooper, NASA/LaRC, Hampton, VA

Program Manager: Jack E. Harrison, Boeing Aerospace Co., Seattle, WA

16. Abstract

A test program was conducted to evaluate standard single lap, double lap and symmetric step-lap bonded joints of Celion 3000/PMR-15 graphite/polyimide composite. Composite-to-composite and composite-to-titanium joints were tested at 116K (-250°F), 294K (70°F) and 561K (550°F). Joint parameters evaluated were lap length, adherend thickness, adherend axial stiffness, lamina stacking sequence and adherend tapering. Tests of advanced joint concepts were also conducted to establish the change in performance of preformed adherends, scalloped adherends and hybrid systems. Special tests were conducted to establish material properties of the high temperature adhesive, designated A7F, used for bonding. Most of the bonded joint tests resulted in interlaminar shear or peel failures of the composite. There were very few adhesive failures. Average test results agree with expected performance trends for the various test parameters. Results of finite element analyses and of test/analysis correlations are also presented.

17. Key Words (Suggested by Author(s)) Composite Composite joints Bonded joints Graphite/Polyimide Celion 3000/PMR-15	18. Distribution Statement Unclassified - Unlimited Subject Category 39
19. Security Classif. (of this report) Unclassified	20. Security Classif. (of this page) Unclassified	21. No. of Pages 78	22. Price A05

REFERENCES

1. Sheppard, C.H.; Hoggatt, J.T.; and Symonds, W.A.: Quality Control Development for Graphite/PMR-14 Polyimide Composite Materials. NASA CR-159182, 1979.

2. St. Clair, T.L.; and Progar, B.J.: LARC-13 Polyimide Adhesive Bonding. SAMPE Series Volume 24 - The Enigma of the Eighties: Environment, Economics, Energy. San Francisco. May 1979, pp. 1081-1092.

3. Cushman, J.B.; and McCleskey, S.F.: Design Allowables Test Program, Celion 3000/RMR-15 and Celion 6000/PMR-15 Graphite/Polyimide Composites. NASA CR-165840, 1982.

4. Sawyer, James Wayne; and Cooper, Paul A.: Analysis and Test of Bonded Single Lap Joints with Preformed Adherends. AIAA/ASME/ASCE/AHS 21st Structures, Structural Dynamics and Materials Conference. May 1980, pp. 664-673.

5. Hart-Smith, L.J.: Adhesive-Bonded Single-Lap Joints. NASA CR-112236, January 1973.

6. Goland, M.; and Reissner, E.: The Stresses in Cemented Joints. Journal of Applied Mechanics, Vol. 11, No. 1, March 1944, pp. A17-A27.

7. Hart-Smith, L.J.: Adhesive-Bonded Scarf and Stepped-Lap Joints. NASA CR-112237, January 1973.